# Logical analysis of the budding yeast cell cycle

D.J. Irons




Logical analysis of the budding yeast cell cycle

D.J. Irons

PII: S0022-5193(08)00661-9
DOI: doi:10.1016/j.jtbi.2008.12.028
Reference: YJTBI5410

To appear in: *Journal of Theoretical Biology*

Received date: 23 May 2008
Revised date: 15 December 2008
Accepted date: 16 December 2008

Cite this article as: D.J. Irons, Logical analysis of the budding yeast cell cycle, *Journal of Theoretical Biology* (2009), doi:10.1016/j.jtbi.2008.12.028

# Logical analysis of the budding yeast cell cycle

D.J. Irons *

*School of Mathematics and Statistics, University of Sheffield, United Kingdom*

**Abstract**

The budding yeast *Saccharomyces cerevisiae* is a model organism that is commonly used to investigate control of the eukaryotic cell cycle. Moreover, because of the extensive experimental data on wild type and mutant phenotypes, it is also particularly suitable for mathematical modelling and analysis. Here, I present a new Boolean model of the budding yeast cell cycle. This model is consistent with a wide range of wild type and mutant phenotypes and shows remarkable robustness against perturbations, both to reaction times and the states of component genes / proteins. Because of its simple logical nature, the model is suitable for sub-network analysis, which can be used to identify a four node core regulatory circuit underlying cell cycle regulation. Sub-network analysis can also be used to identify key sub-dynamics that are essential for viable cell cycle control, as well as identifying the sub-dynamics that are most variable between different mutants.

*Key words:* Yeast cell cycle, Boolean models, Modularity, Networks



## 1 Introduction

The eukaryotic cell cycle corresponds to the events underlying cell proliferation, whereby a single cell grows and divides into two daughter cells. The first main phase in the cell cycle is S phase where DNA synthesis occurs and each chromosome is replicated to give two identical sister chromatids. After DNA synthesis, the cell enters *mitosis* (M phase), with the DNA condensing and the chromosomes aligning themselves on the centre of the mitotic spindle (*metaphase*). The mitotic spindle forms during the cell cycle from fibres called microtubules, each microtubule connected to one of the two poles of the cell. The microtubules attach themselves to sister chromatids, which are then

* Corresponding author.
*Email address:* d.irons@sheffield.ac.uk (D.J. Irons ).

pulled apart, with one copy being sent to each pole (*anaphase*). Finally, the cell divides into two smaller cells, each with one copy (*telophase*). Generally, the cell cycle can be considered as two main phases S phase (DNA synthesis) and M phase (Mitosis; consisting of metaphase, anaphase and telophase), which are separated by gap phases G1 and G2 (i.e. we have G1 $\rightarrow$ S $\rightarrow$ G2 $\rightarrow$ M $\rightarrow$ G1). To ensure safe passage through cell cycle, there are a number of checkpoints that are built into the regulatory process, which monitor features such as cell size, shape, spindle alignment and DNA damage.

Of all the eukaryotic cell cycles, that of the budding yeast *Saccharomyces cerevisiae* has been one of the most extensively studied and characterised, both from an experimental and modelling perspective. In particular, many studies have looked at the temporal regulation of the main genes and proteins, as well as the main interactions involved (for reviews see Bähler (2005); Wittenberg & Reed (2005); Bloom & Cross (2007)). *S. cerevisiae* differs slightly from other eukaryotes in the way the cell grows during the cell cycle. As the cell grows, a bud forms from the side of the cell and holds one pole of the mitotic spindle. The bud then eventually becomes the daughter cell, after cell division, with one copy of the genetic material being sent there during anaphase (the original cell is called the mother cell).

In the past, mathematical models of the *S. cerevisiae* cell cycle have been produced, using both ordinary differential equations (ODEs) and Boolean network models. In Chen *et al* (2000, 2004), comprehensive ODE models have been produced that incorporate detailed molecular concentrations and reactions for each mRNA / protein, and are consistent with a significant amount of wild type and mutant data. Further detailed models have then also been produced that focus on the transition from G1 to S phase (Barberis *et al* (2007)) and mitotic exit (Queralt *et al* (2006); Tóth *et al* (2007)). One problem with ODE models is that detailed analysis can be difficult for systems with a large number of genes and proteins. Moreover, for large models, there is a large number of unknown parameters that need to be estimated. Therefore it is also of interest to have simpler models that allow the main qualitative features of the system to be analysed more easily. On this count, Boolean network models (where each gene / protein is represented as ON or OFF) provide a less computationally intensive alternative for analysing the logical structure of the system. A Boolean model of this system has been previously proposed by Li *et al* (2004), which captures the wild type dynamics and shows remarkable robustness to the exact timings of individual interactions (Braunewell & Bornholdt (2007)). However, this model does not explicitly model mitotic exit and is inconsistent with a number of mutant phenotypes. Beyond *S. cerevisiae*, more generic cell cycle models have also been created that look at fission yeast, frog eggs and mammalian cells (Csikász-Nagy *et al* (2006); Fauré *et al* (2006)).

To account for 'noise' in the yeast cell cycle, stochastic models have also been

produced. These approaches include adapting ODE models to give Stochastic Petri Net models (Mura & Csikász-Nagy (2008)) and Langevin-type equations (Steuer (2004)). Meanwhile, the existing Boolean model of Li *et al* (2004) has also been adapted to allow random variations in in process times (Zhang *et al* (2006); Braunewell & Bornholdt (2007)).

In Section 3 of this paper, I present a new Boolean network model for the *S. cerevisiae* cell cycle, which incorporates knowledge from both the existing models and the current literature. The results from this model are now consistent with a wide range of wild type and mutant phenotypes (Section 4). Moreover, because of the qualitative nature of the model, I have been able to isolate interesting sub-dynamics associated with the viable wild type and mutant phenotypes (in Section 5). This model is not designed to replace existing continuous models, but rather summarise existing knowledge of the *S. cerevisiae* cell cycle and show that logical functions and Boolean states can capture the essential features of the system. First, in Section 2, I formally introduce Boolean network models and some new adaptations that are used in the model.



## 2 Boolean network models and non-uniform time delays

A Boolean network model is a dynamical system consisting of a network of $v$ nodes $V = \{n_1, ..., n_v\}$, each of which has a Boolean state $s_i \in \{0, 1\}$ (OFF or ON). The system progresses over time by nodes updating their states according to logical rules called Boolean functions. So, if a node $n_i$ is due to update at time $t$, its state changes according to a Boolean function $f_i$ as follows

- $s_i(t) = f_i(\mathbf{x}^{N_i}(t-1))$

Here, $N_i$ is the set of nodes with outgoing edges to $n_i$ and $\mathbf{x}^{N_i}(t-1)$ is the state of those nodes at the previous time step. $f_i$ then converts $\mathbf{x}^{N_i}(t-1)$ into a Boolean state (0 or 1). For example, for the node $n_4$ in Fig.1B, $N_4 = \{n_1, n_2, n_3\}$ and a possible Boolean function can be seen in Table 1. It is also possible to have discrete logical models by allowing nodes to take discrete states 0,1,2,3 ... instead of just 0 or 1.

In the simplest case, all nodes are deterministically and *synchronously* updated at each time step $t$. Then, as time progresses, the state of the network $\mathbf{x}(t) = \{s_1(t), ..., s_v(t)\}$ eventually settles to a stable state called an *attractor* $A = \{\mathbf{z}_0, ..., \mathbf{z}_{p-1}\}$. i.e. there is a time point $t'$ for which

- For all $t \geq t'$, $\mathbf{x}(t) = \mathbf{z}_k \quad (\text{where } k = t - t' \pmod p)$.

For a given model, there are typically multiple attractors, which can either be cyclic ($p > 1$) or fixed point attractors ($p = 1$, i.e. $\mathbf{x}(t) = \mathbf{x}(t')$ for every $t \geq t'$).

Alternatively, nodes can be updated *asynchronously* and / or *stochastically*. In the most impartial case, a single node is chosen at random (to update) at each time step. However, more biologically feasible schemes have also been proposed that assign variable time units to each node. For example, Chaves *et al* (2006) have proposed a scheme where each node $n_i$ has a time parameter $\gamma_i$, corresponding to a reaction speed. The updating times are then pre-specified as $T_{i_1}$, $T_{i_2}$, ..., $T_{i_k}$, ..., where $T_{i_{k+1}} = T_{i_k} + \gamma_i = k\gamma_i$. With these asynchronous / stochastic updating schemes, the fixed point attractors will be the same as those in the default Boolean network model. This is because, once the system fixes itself at a single state, any single node update will leave the whole network state unchanged, and so the update order makes absolutely no difference. However, there are likely to be differences in the cyclic attractors and trajectories to attractors in general. To look at these models in a continuous time framework, Boolean models have also been adapted to form piecewise linear ODE models (e.g. Chaves *et al* (2006); Braunewell & Bornholdt (2007)).

Boolean network models and discrete logical models, using a variety of updating schemes, have been used to successfully study various genetic regulatory systems (e.g. Mendoza & Alvarez-Buylla (1998); Albert & Othmer (2003); Li *et al* (2004); Chaves *et al* (2005); Fauré *et al* (2006); Li *et al* (2006); Braunewell & Bornholdt (2007)) and each scheme has its advantages and disadvantages. One issue of particular importance in many systems is the timing of updates, since biological interactions can take place over a large range of time scales. For example, protein-protein interactions and nuclear transportation are very quick compared to transcription and translation. Another regulatory process that does not occur within a narrow time band is protein degradation, often taking different lengths of time for different proteins and environmental conditions. In theory, asynchronous or stochastic updating schemes are ideally suited to this problem as the times between updates can vary between nodes. However, having a deterministic and synchronous updating scheme is more suitable for analysis by algorithms that (1) identify every attractor (both fixed point and cyclic) and (2) identify functional sub-dynamics (Irons (2006); Irons & Monk (2007)). Moreover, when producing a new model, a synchronous updating scheme provides a set of baseline results, to which more complicated updating schemes can be compared.

In order to have a range of interaction timescales, whilst maintaining the computational and analytical advantages of a deterministic synchronous updating scheme, I propose a new technique that introduces 'dummy' nodes into a Boolean network model. This technique is summarised below and described in detail in Appendix A. An accompanying example, can be seen in Fig.1 and

Table 2.

Consider a node $n_b$ and suppose a set of neighbouring nodes $N_a = \{n_{a_1}, ..., n_{a_k}\}$ is involved in activating it when when they satisfy a logical condition $IN$. For example, in Fig.1C and Table 2, the logical condition used is $IN = (s_1 = 1 \text{ OR } s_2 = 1)$. Then, the addition of $'r'$ dummy nodes allows the model to hold a record of this 'signal' $IN$ over an additional $'r'$ time steps and delay it reaching $n_b$. In this paper, I use this system to introduce *activation* and *degradation* delays to model (relatively) slow transcription and degradation.

**A. Activation delay**
The set of nodes $N_a$ must satisfy $IN$ for $r_A$ continuous time steps (rather than the usual 1), in order for it to have an activating effect on $n_b$.

**B. Degradation delay**
If $n_b$ is already ON, then the activating effect due to $N_a$ remains until $IN$ is not satisfied for $r_D$ continuous time steps (rather than the usual 1).

Once $r = \max\{r_A - 1, r_D - 1\}$ dummy nodes have been added to the model, Boolean functions can be adapted to incorporate both of these types of delay (as described in Appendix A). I note here that the delay is added specifically to the signal $IN$. Therefore, the node set $N_a$ need not be the full set of inputs for $n_b$. It could also be the case that other signals $\mathbf{y}^{M_a}$, to the same node, are subject to different delays.

Without delays, Boolean network models are a logical description of how each node (gene, protein or event) is regulated, and so they do not have parameters per se (at least not in the same way as differential equation models). However, with the addition of activation and degradation time delays there are now $2\sum_{k=1}^{v} I_k$ parameters, where $I_k$ is the number of interactions or signals regulating node $n_k$. Returning to the example in Fig.1 and Table 2, there are two 'signals' $IN_1 = (s_1 = 1 \text{ OR } s_2 = 1)$ and $IN_2 = (s_3 = 0)$ regulating $n_4$ and so $I_4$ would be 2. However, other logical combinations of nodes $n_1$, $n_2$ and $n_3$ could give rise to more or less signals.



## 3 Boolean network model of the yeast cell cycle

In this section, I introduce a new Boolean model for the *S. cerevisiae* cell cycle. The model consists of 18 nodes with the Boolean functions shown in Table 3. Four of the nodes 'S', 'B', 'M' and 'CD', represent cell cycle events 'DNA synthesis', 'Bud growth', 'entry into Mitosis' and 'cell division' (resp). The remaining 14 nodes represent groups of genes and proteins, involved in cell cycle regulation. Often, an individual node corresponds to more than one gene / protein, whose functions are related (see Table 4 for breakdown).

In order to summarise cell cycle regulation and justify the Boolean functions used in the model, this section describes and justifies the main interactions involved (highlighted as **A** - **Y**). As can be seen in Table 3, individual nodes can be regulated by many interactions over different timescales (which occur in different phases of the cell cycle). How these interactions combine to give the Boolean functions, and the time delays used, is discussed further in Section 3.2.

### *3.1 Summary of main interactions*

As mentioned previously, the cell cycle has 4 main phases G1, S, G2 and M. In summary, the transitions into S phase and M phase are induced by cyclins Cln1-3 and Clb1-6, bound to the main cyclin dependent kinase Cdc28 (in the model and justifications below, these are represented by *Cln2*, *Cln3*, *Clb2* and *Clb5*). Cyclin inhibitors such as Cdc20, Cdc14, CKI and Cdh1 then become active in M phase, promoting cyclin degradation, mitotic exit and a return to G1 phase.

Below, I describe the main interactions involved in cell cycle regulation, in terms the four transitions illustrated in Fig.2. Where a node is involved in an interaction, but is not responsible in that phase of the cell cycle, it is marked with a star ($\star$).

#### *3.1.1 Transition from G1 to S phase (Fig.2A)*

Once a new cell cycle begins, Cln3 sets off a chain of interactions that leads to the activation of Cln2, Clb5 and the degradation of cyclin-dependent kinase inhibitors (CKI). This then promotes the transition into S phase by promoting DNA synthesis (S) and Bud formation (B) .

***A:*** *Cln3 or Cln2 can activate S/MBF*
***B:*** *S/MBF activates Cln2 and Clb5*

Once Cln3 levels rise above some threshold it activates two transcription factor complexes SBF (Swi6-Swi4) and MBF (Swi6-Mbp1) (both part of the S/MBF node), by removing the antagonist Whi5 from the nucleus (Costanzo *et al* (2004); Wittenberg & Reed (2005)). SBF and MBF then transcribe a set of target genes that promote DNA synthesis and Bud formation; including CLN2 and CLB5 (Wittenberg & Reed (2005); Bähler (2005)). Cln2 is also capable of activating SBF and MBF, by antagonising Whi5 (Costanzo *et al* (2004); Wittenberg & Reed (2005)).

***C:*** *Cln2, Clb5 or Clb2$^\star$ can inhibit CKI*

***D:*** *Cln2, Clb5 or Clb2* can inhibit Cdh1*

Once Cln2 levels build up they inhibit CKIs (such as Sic1) by promoting their phosphorylation and degradation (Verma *et al* (1997); Nash *et al* (2001)). In wild type cells, CKI inhibition of Clb5 is then released, allowing Clb5 levels to rise. Clb5 and Clb2 have also been shown to trigger Sic1 degradation (Verma *et al* (1997)), and so these additional interactions are included in the model. Cln2, Clb5 and Clb2 have also been shown to phosphorylate and inhibit another key protein Cdh1 (also known as Hct1) from late G1 to M phase (Zachariae *et al* (1998)).

***E:*** *Clb5 and Clb2* activate S*
***F:*** *Cln2 and Clb5 activate B*

Cln2 and Clb5 also promote Bud formation and DNA synthesis. Clb5 is primarily associated with initiating DNA replication but, in its absence, other Clb's (e.g. Clb2) can initiate S phase once they are expressed (Schwob & Nasmyth (1993); Hu & Aparicio (2005)). Bud formation is initiated by Cln2 but under certain conditions Clb5 have also been shown to be important (Cvrčková & Nasmyth (1993); Epstein & Cross (1992); Li & Cai (1999)).

***G:*** *S/MBF activates Yhp1*
***H:*** *Yhp1 inhibits Cln3*

In G1 and S phase, SBF is also responsible for transcribing other important genes, including YOX1 (directly) and YHP1 (indirectly through Hcm1) (Horak *et al* (2002); Bähler (2005); Pramila *et al* (2006)). In the model *Yhp1* corresponds to the two proteins Yox1 and Yhp1 that inhibit Cln3 up until late M phase. When neither of these inhibitors are present (between M phase and early G1), CLN3 transcription is activated by a protein Mcm1 that is assumed present throughout the cell cycle (Wittenberg & Reed (2005); Bähler (2005)).



### *3.1.2 Entry into mitosis (Fig.2B)*

Following Bud formation, Clb2 becomes active and promote entry into mitosis (M).

***I:*** *Clb2 and SFF activate one another*
***J:*** *B activates Clb2 and SFF*

In G2 phase, CLB2 is activated by the transcription factor complex SFF (consisting of the proteins Fkh2 and Ndd1) that function alongside Mcm1. (Maher *et al* (1995); Wittenberg & Reed (2005); Bähler (2005)). Under normal conditions, Mcm1 and Fkh2 are assumed present throughout the relevant

phases of the cell cycle, and the crucial regulatory step is the recruitment of Ndd1, which primarily requires Clb2 itself (Wittenberg & Reed (2005); Bähler (2005)). Therefore, in the absence of inhibition, low levels of Clb2 can activate a positive feedback loop that is capable of maintaining its activation.

However, even after CKIs and Cdh1 have been degraded in G1 phase, another inhibitor Swe1 can still prevent full Clb2 activity. Once the bud has grown to a critical size and shape, Swe1 is localised to the bud neck and degraded (promoted by low but increasing levels of Clb2) (Lew (2003); Lee *et al* (2005); Hood-DeGrenier *et al* (2007)). Therefore, in the model, Clb2 and SFF are not initially activated until Bud formation has occurred.

***K:*** *Clb2 and S are necessary for M*

The main protein responsible for promoting mitotic entry is Clb2 (Surana *et al* (1991); Richardson *et al* (1992); Bloom & Cross (2007)). Therefore, once DNA synthesis has occurred and Clb2 is active, the chromosomes will be aligned on the mitotic spindle, signalling entry into mitosis.

***L:*** *SFF is necessary for Cdc20 and Swi5 activity*
***M:*** *Clb2 inhibits S/MBF and Swi5*

Once SFF and Clb2 are active, they also play a role in regulating other cell cycle proteins involved in M phase. SFF transcriptionally activates CDC20 and SWI5 (Lydall *et al* (1991); Wittenberg & Reed (2005)). However, the Swi5 protein is then phosphorylated and removed from the nucleus because of Clb2 activity (Bähler (2005)). Clb2 also leads to the inhibition of G1 / S phase proteins by inhibiting SBF (Wittenberg & Reed (2005)).

### *3.1.3 Transition through M phase and execution of anaphase (Fig.2C)*

After mitotic entry, Cdc20 becomes functionally active and triggers a chain of events that activates two important mitotic pathways, FEAR ('Cdc Fourteen Early Anaphase Release') and MEN ('Mitotic Exit Network'). MEN and FEAR co-operate to release Cdc14, which then co-operates with FEAR components (including Separase) to execute the transition into anaphase; with functions including spindle stability and sister chromatid separation.

***N:*** *M and Clb2 are necessary for Cdc20 activity*

Once the chromosomes are correctly aligned on the mitotic spindle, Cdc20 is released (from inhibition by MCM) and activates APC (Anaphase Promoting Complex) (Hwang *et al* (1998); Musacchio & Salmon (2007)). Therefore, for this node to be active, the cell must have successfully entered mitosis (i.e. M = 1). Moreover, phosphorylation by Clb2 has also been shown to be necessary

for Cdc20-APC activation (Rudner & Murray (2000)).

***O:*** *Cdc20 inhibits Clb5*
***P:*** *Cdc20 activates FEAR*
***Q:*** *FEAR and Clb2 combine to activate MEN*

Once active, Cdc20-APC leads to the degradation of Clb5 and Pds1 (Shirayama *et al* (1999)). The degradation of Pds1 (Securin) then leads to the activation of the FEAR pathway and the release of Eps1 (Separase), which promotes sister chromatid separation (D'Amours & Amon (2004)). FEAR and Clb2 then combine to activate the MEN signalling cascade (via Tem1). Clb2 activates Cdc5 (Mortensen *et al* (2005)), which then combines with the FEAR component Esp1 to down-regulate MEN inhibitors PP2A and Bub2-Bfa1 (Hu *et al* (2001); Queralt *et al* (2006)).

***R:*** *FEAR and MEN activate Cdc14*

Once FEAR and MEN pathways are both active, they combine to activate Cdc15 and Cdc14 (Stegmeier *et al* (2002); D'Amours & Amon (2004)). During most of the cell cycle Cdc14 is inactive and bound to an inhibitor Net1. The FEAR network causes a (relatively) small amount of Cdc14 to be released into the nucleus, by inhibiting PP2A (Queralt *et al* (2006)). This small amount of Cdc14, along with components of the MEN pathway, then lead to the activation of Cdc15. Cdc15 then promotes Cdc14 release throughout the cell.

#### *3.1.4 Exit from mitosis (Fig.2D)*

Once Cdc14 is active, it triggers a number of interactions that result in cell division and prepare the cell for the subsequent cycle and G1 phase.

***S:*** *Cdc14 activates Cdh1, Swi5 and CKI*
***T:*** *Swi5 activates CKI*

Cdc14 can de-phosphorylate and activate Cdh1-APC, Swi5 and Sic1 (CKI) (Visintin *et al* (1998)). In the case of Swi5, this dephosphorylation allows Swi5 to return to the nucleus, where it can activate target genes including SIC1 (Visintin *et al* (1998); Bähler (2005)). The de-phosphorylation of Sic1 by Cdc14 then protects it from degradation and allows levels to accumulate.

***U:*** *Cdh1 and Cdc20 co-operate to inhibit Clb2*
***V:*** *CKI inhibits Clb2 and Clb5*$^{\star}$

The activation of Cdh1 and CKI also help prepare for cell division and the subsequent G1 phase by inhibiting Clb2. Cdh1-APC and Cdc20-APC act co-

operatively to degrade Clb2. Cdc20-APC reduces Clb2 to low / medium levels, whereas Cdh1 can degrade low levels of Clb2 (Yeong *et al* (2000); Cross *et al* (2002); Potapova *et al* (2006)). Meanwhile CKIs, such as Sic1, can bind and inhibit Clb2 and Clb5 (Schwob *et al* (1994)), keeping their levels low.

***W:*** *M, FEAR and Cdc14 are all necessary for CD*
***X:*** *CD resets S, B, M and CD*

The exact processes underlying cell division itself are still not completely understood. However, cell division is dependent on mitotic entry (M), FEAR and Cdc14, since they are essential for completing anaphase and providing a safe passage to mitotic exit (D'Amours & Amon (2004)). The inhibition of Clb2 has also been associated with mitotic exit, but its complete degradation is not essential (Wäsch & Cross (2002)). Instead, early phase (partial) degradation due to Cdc20-APC is sufficient. Therefore, since (1) Cdc20-APC is essential for FEAR activity and (2) FEAR forms part of the Boolean function, we do not include Clb2 in this function. In the model, once Cell Division (CD) has occurred, the states of S, B and M are reset to 0 for the next cell cycle (by allowing the CD node to inhibit them).

### *3.2 Construction of Boolean functions and timing of interactions*

The Boolean functions in Table 3 are a logical description of the interactions **A** to **X** described above, along with some additional interactions (**Y**) that ensure certain nodes remain active after the initial source of activation has disappeared. This is the case for CKI and S/MBF where extra self interactions are put in the model to ensure they are are active up until an inhibitor is present (as in wild type cells). Similar self interactions are put in the model to maintain the event nodes B, S and M until Cell Division occurs.

***Y:*** *S/MBF, CKI, S, B and M can all maintains their own activity in the absence of inhibitors.*

The Boolean functions are represented by the second column of Table 3. Here, each row represents a condition (at time $t-1$) that leads to that node taking state 1 a time $t$. If no such condition is met for a particular node then it takes state 0 at time $t$. To see how the the interactions **A** to **Y** combine to give the Boolean functions, consider the case of Clb2.

Here, interaction **I** or **J** can lead to Clb2 activation, when it is NOT being inhibited via interactions **U** or **V**. Therefore, since conditions (a) CKI = 0 AND Cdh1 = 0 and (b) CKI = 0 AND Cdc20 = 0 ensure **U** and **V** can't take place and conditions (c) B = 1 and (d) Clb2 = 1 AND SFF = 1 ensure **I** or **J** can take place, we get the four conditions in the Boolean function (a + c, b

+ c, a + d, b + d).

### *3.2.1 Timing of interactions*

Most interactions, such as protein-protein interactions and activation / inactivation by phosphorylation or dephosphorylation, are assumed to take just 1 time step in the model. However, other interactions corresponding to transcription, degradation or cell cycle events (B,S and M) take longer and are subject to time delays. If $'\ [condition]\{r_A : d_A\} = c\ '$ appears in a Boolean function $f_i$ (for a node $n_i$) then that interaction is subject to activation / degradation times of $r_A$ /$d_A$ respectively (described in Section 2 and Appendix A). Below, I explain and justify the occurrence of each delay.

In the model, transcriptional activation of nodes is assumed to take 2 time steps. In particular

- Cln3 activity in response to Yhp1,
- Cln2, Clb5 and Yhp1 activity in response to S/MBF,
- Cdc20 and Swi5 activity in response to SFF,
- CKI activity in response to Swi5 (and Cdc14).

However, there are still a couple of exceptions to this general rule. Firstly, in the continued presence of CKI, Clb5 and CKI mutually inhibit one another and it takes longer for Clb5 levels to build up and become functionally active (4 time steps). Secondly, since the activity of Clb2 and it's transcription factor SFF are dependent on one another, I assume that they both activate simultaneously following bud formation (1 time step). Initial activation of the cell cycle event nodes are also subject to activation delays. In the case of S, M and CD, this delay is assumed to take 2 time steps. However the completion of bud formation (B) is assumed to take significantly longer (6 time steps). The activity of the B node corresponds to the bud reaching a critical size and the degradation of Swe1. In wild type cells, this occurs in G2 phase (after DNA synthesis) and so we assume that it takes longer than DNA synthesis in the model.

In most cases, the inactivation of nodes (due to inhibition or removal of activators) takes 1 time step. However, where protein degradation is a cause for node inactivation, the time scales are allowed to vary depending on the evidence available. In the case of Cln3, Cln2 and Cdc20, degradation is assumed to be quick after transcription stops (1 time step) due to the fact that Cln3 and Cdc20 are unstable (Tyers *et al* (1992); Prinz *et al* (1998); Wittenberg & Reed (2005)) and the protein complex SCF, responsible for Cln2 degradation, appears to be present throughout the cell cycle (Willems *et al* (1996)). Meanwhile, in the absence of inhibition, Clb5 and Swi5 degradation is assumed to be slower (3 time steps) since the respective proteins are present in the cell

after transcription has ended (Shirayama *et al* (1999); Bähler (2005))

For Yhp1, the precise mechanisms promoting the late expression of YHP1 remain unknown and so we allow this nodes activity to persist for $3 + 3 = 6$ time steps after the S/MBF has disappeared. In support of this approach YHP1 expression is partially due to Hcm1, which is itself a target of SBF (Pramila *et al* (2006)). Therefore, Yhp1 would only begin to degrade after Hcm1 had degraded (which would be some time after the inactivation / disappearance of SBF). Moreover, this approach ensures that Yhp1 is active in the correct phases of the cell cycle (S phase to early M phase; Spellman *et al* (1998)). More research will be required to fully understand how Yhp1 is regulated.

## 4 Wild type, mutant and checkpoint attractors

### *4.1 Validation and robustness of model*

In order to demonstrate that the model is applicable to the *S. cerevisiae* cell cycle, I show that the stable dynamics (attractors) are consistent with experimentally observed wild type and mutant phenotypes. The wild type model is the above mentioned model, described in Table 3. In appropriate extra-cellular conditions, wild type cells will go through S and M phase before dividing into two. This process will then be repeated with the new cells, and so on. Therefore, when testing the model, I assume an attractor is viable if the cell cycle event nodes (S, M and CD) are all activated in order (before returning to G1 phase where S,M and CD are all off). This is the case for the main wild type attractor in Fig.3A.

As verified by the algorithm in Irons (2006), Fig.3A is the only attractor for the wild type model (fixed or cyclic). Therefore, the model indicates that the system is remarkably robust to both perturbations in gene / protein activity and variations in reaction times. Firstly, any perturbation to any node (i.e. artificially turning a node ON or OFF for a finite period of time) cannot push the system into a different stable trajectory / attractor, since none exist. In a similar way, changes to the way nodes are updated or the timing of individual interactions will not fundamentally change the stable dynamics. This can be seen in Fig.3B, which shows that you get an analogous attractor when all additional time delays are removed from the model. Although the timing of activation / deactivation of certain nodes is shifted, the relative order of the most important changes are preserved (e.g. S/MBF, Clb2, Cdc20, FEAR, Cdc14, CKI, S, M, CD). Once again, this is the only attractor for the model. These findings also indicate that the synchronous updating scheme is appropriate in this case and gives a plausible representation of the stable

dynamics.

The model is also consistent with a number of relevant mutant phenotypes. In experiments, a mutant phenotype $'X\triangle'$ corresponds to protein $'X'$ being inactivated, often by a mutation to the corresponding gene. In order to test the ability of the model to replicate mutant phenotypes, I have looked at the effect of permanently fixing node states (Table 6) to see how the dynamics compare with experimental observations, for appropriate mutations (Table 5). Clb2 and SFF are grouped together because the activation of SFF is tied to that of Clb2 in the model. For each mutant, the main attractor can be seen in Fig.4.

One thing that is clear, by comparing Table 6 to Table 5, is that the main attractor associated with each mutant compares well with the experimentally observed phenotype. All 6 viable mutants are viable in the model and the observations relating to the length of G1 phase are replicated. i.e. fixing Clb5 to 0 leads to a longer G1 phase (+4 time steps), whilst fixing Yhp1, Swi5 or CKI to 0 leads to a shorter G1 phase ($-1$, $-2$, $-2$ time steps respectively). The 7 inviable mutants are also replicated by the model, with the resulting attractors corresponding to the correct phases of the cell cycle. Fixing Cln3 or S/MBF to 0 leads to an attractor for which the nodes S, M and CD are all 0. This correctly corresponds to the cell arresting in G1 phase. When, fixing Clb2 / SFF to 0, the main attractor correctly corresponds to a G2 cell cycle arrest with S = 1 and M, CD both equal to 0. From experimental data Cdc20$\triangle$, Esp1$\triangle$, Tem1$\triangle$, Cdc15$\triangle$ and Cdc14$\triangle$ all lead to the cell arresting during mitosis, although slightly different stages of mitosis. In the model, the corresponding attractors have S = 1, M = 1 and CD = 0 corresponding to the cell entering mitosis but then never being able to promote cell division. This is again consistent with the experimental data.

Additionally, as in wild type case, changes to the way that nodes are updated or to the timing of individual interactions does not fundamentally change the mutant attractors. This can be seen in *Supporting Figure 1*, which shows that analogous mutant attractors are obtained when all additional time delays are removed from the model. Moreover, for each of the viable mutants, there is only a single attractor and so those attractors will also be robust to perturbations.

These results indicate that both the *S. cerevisiae* cell cycle and this model show a remarkable degree of robustness. The presence of 6 (out of 13) viable mutants show that the system can still maintain its primary function when any one of these 6 nodes are inactivated / removed. This is primarily because there is a lot of redundancy in the system, with alternative pathways available when one protein is absent. For example, when Clb5 is absent, DNA synthesis can still occur because of an alternative pathway involving Clb2.

### *4.2 Checkpoint attractors*

Although the wild type model only has a single attractor, cells can temporarily halt their progression though the cell cycle when certain 'checkpoints' are activated. For the wild type model, the responses to six different checkpoints were simulated by fixing the states of the genes / proteins being regulated (Fig.5). In each case the figure shows the main attractor associated with each checkpoint.

The *start checkpoint* is responsible for regulating the G1 - S phase transition, ensuring that S phase does not begin until the cell reaches some critical size. Although the precise mechanism linking S phase initiation to cell size remains unclear, two proteins, Far1 and Whi5, keep the cells in G1 by inhibiting Cln3 and SBF respectively (McKinney *et al* (1993); Henchoz *et al* (1997); Costanzo *et al* (2004); de Bruin *et al* (2004)). The checkpoint is then lifted once Cln3 levels are high enough to first overpower Far1 and then remove Whi5 from the nucleus. Ribosome biogenesis is also monitored by and affects this checkpoint, by regulating Whi5 (Bernstein *et al* (2007)). The response to this checkpoint can be seen in Fig.5A by fixing Cln3 to 0 (which also ensures S/MBF is 0 in the model).

The *morphogenesis checkpoint* is also a size checkpoint, this time ensuring the bud has grown to the correct size and shape before the cell enters mitosis. The main protein in this checkpoint is Swe1, which blocks entry into mitosis by inhibiting Clb2 (Lew (2003); Lee *et al* (2005); Hood-DeGrenier *et al* (2007)). Once the bud is adequately formed and Clb2 levels begin to rise, Swe1 is then localised to the bud neck and degraded. The response to this checkpoint can be seen in Fig.5B by fixing node B (Budding) to 0.

Once the cell has entered mitosis, two *spindle checkpoints* exist that prevent anaphase and mitotic exit until the chromosomes and mitotic spindle are correctly aligned. The first checkpoint is active until the sister chromatids are correctly aligned on the mitotic spindle. Before all of the chromosomes are correctly orientated and the kinetochores are attached to the spindle poles, a protein complex MCM (involving Mad2) inhibits Cdc20 (Hwang *et al* (1998); Musacchio & Salmon (2007)). However, once the chromosomes are correctly aligned, Cdc20 is released and activates APC/C (Anaphase promoting complex). The response to this checkpoint can be seen in Fig.5C by fixing Cdc20 to 0. A second spindle checkpoint is active until the mitotic spindle is correctly aligned. Here, Bub2 / Bfa1 inactivates the MEN protein Tem1 until the spindle begins to elongate and the daughter bound Spindle Pole Body enters the bud, where Tem1 will be spatially located with it's activator Lte1. (Fraschini *et al* (1999); Alexandru *et al* (1999); D'Amours & Amon (2004)). The response to this checkpoint can be seen in Fig.5D by fixing MEN to 0.

Finally, *DNA damage checkpoints* exist that are capable of delaying both S phase and mitotic exit. In response to DNA damage, Rad53 been shown to phosphorylate Swi6 in G1 / S phase thus inhibiting SBF (Sidorova & Breeden (1997)). The response to this checkpoint can be seen in Fig.5E by fixing S/MBF to 0. In M phase, DNA damage activates Chk1 and Rad53 pathways that results in the inhibition of FEAR and MEN respectively, thus preventing Cdc14 release (Liang & Wang (2007)). The response to this checkpoint can be seen in Fig.5F by fixing both FEAR and MEN to 0.

## 5 Sub-network analysis of model

Because of its deterministic logical nature, it has been possible to analyse this new model to identify informative sub-networks and sub-dynamics within the cell cycle. Irons & Monk (2007) proposed a method for identifying subsystems in Boolean network models. In this method, a subsystem is (by definition) a dynamical feature of the system, rather than just a topological one. Each subsystem is a sub-network along with a state / dynamical process acting on it. In fact, individual nodes could form part of multiple subsystems. This method essentially works by comparing attractors (fixed or cyclic) and looking for subsystems; each one (1) conserved across some set of attractors and (2) distinguishable from the stable dynamics for the rest of the system.

Since the wild type model in this paper only has a single attractor, this method gives a trivial output (the single cell cycle attractor is a subsystem). This seems reasonable because the cell cycle genes and proteins combine to carry out a joint function; namely regulation and timing of the cell cycle events. However, using the checkpoint attractors and mutant attractors, I have been able to use analogous methods to identify interesting sub-dynamics within the cell cycle.

Firstly, as can be seen in Fig.5, looking at a variety of checkpoints gives rise to a further 6 steady states corresponding to natural breaking points in the system. Applying the algorithm from Irons & Monk (2007) to this set of attractors then gives the 13 subsystems in Fig.6A, which cleanly partition the full network into 7 smaller sub-networks. Each of these subsystems corresponds to a state that is maintained across a number of checkpoint attractors whilst having a different activity profile from the remaining nodes. For example, the subsystem where Clb2, SFF, B and M are all ON is maintained across 3 checkpoint attractors (Fig.5C,D and F) but not in the other 3 (Fig.5A,B and E). However, it is impossible to find a different node whose state (ON / OFF) splits the set of attractors in the same way (C,D,F vs A,B,E).

By looking at the main genes / proteins in each of these 7 sub-networks and looking at the interactions between them, it is possible to construct a smaller

model of the cell cycle (Fig.6B). However, by looking at these interactions, it is evident that 3 of the nodes only affect the timing of interactions, rather than whether they happen or not. Firstly, the FEAR and Cdc14 sub-networks form the central part of chain and so will not fundamentally affect the interaction between Cdc20 and CKI sub-networks. Secondly, allowing the S/MBF sub-network to activate itself negates the need for Cln3. This then gives us the network in Fig.6C and Boolean functions in Table 7 that faithfully replicate the core cell cycle dynamics (Fig.6D). This reduced model can be viewed as a core regulatory network for cell cycle control, which underlies and drives the full network.

As can be seen in Tables 5 and 6, the cell cycle is robust against multiple mutations. Therefore, it is also of interest to know what sub-dynamics underlie this robustness and are conserved across the 7 viable wild type and mutant attractors. As discussed in Irons & Monk (2007) and Appendix B, the original method of identifying subsystems is not necessarily applicable to data (attractors) where

**(a)** Many similar cyclic attractors correspond to the same function
**(b)** The primary difference between attractors are external perturbations, such as a mutation

(as is the case with the data from the viable wild type and mutant phenotypes).

However, as described in Appendix B, the method can be adapted to find *dominant sub-dynamics*, which are

**(i)** Conserved across (or occur in) a set of attractors,
**(ii)** More informative than other sub-dynamics, conserved across the same set of attractors

For example, $P_A$ in Fig.7A is a dominant sub-dynamic that is conserved across all 7 viable attractors. By this I mean that the states in $P_A$ cycle in the correct order within all 7 viable attractors (see Definition 3 in Appendix B for a formal definition). Note that the time taken to change from one state (in $P_A$) to the next is not considered since different processes can take different lengths of time under different conditions (compare WT and viable mutant attractors). This sub-dynamic is deemed more informative than any other, which is also conserved across all 7 attractors, because of the number of, and uniqueness of, the nodes involved (see Definitions 5 and 6 in Appendix B).

Applying this new method to the 7 viable attractors identifies 7 dominant sub-dynamics that were conserved across at least 2 attractors. $P_A$ represents the dynamics associated with the main proteins involved in mitotic entry and exit and represents an essential sub-dynamic that is conserved in the wild type and all viable mutants. More interesting perhaps is the sub-dynamic $P_B$,

which is conserved across 6 out of the 7 viable attractors (all except the Cdh1 mutant). This sub-dynamic captures the full transition through M phase and anaphase, ending in cell division. Although Cdh1 is not essential for cell cycle transition, the dynamics through mitotic exit are significantly altered because of it. With Cdh1, all of the M phase proteins become active and then inactive in a regimented order. However, without Cdh1 the inhibition of Clb2 is delayed meaning that inactivation of many of the M phase proteins is delayed with respect to the timing of mitotic exit. The remaining 5 dominant sub-dynamics are all conserved across fewer attractors but involve a wider variety of nodes.

These dominant sub-dynamics can also be used to see what sub-dynamics are tightly / uniquely associated with each mutant; by finding the nodes within each attractor that aren't part of any dominant sub-dynamic occurring within that attractor. Table 8 shows the nodes whose sub-dynamics are uniquely associated with each mutant attractor. One interesting thing to note is that the dynamics for both Clb5 and CKI are uniquely associated with all viable mutants. These nodes are primarily responsible for the transition from G1 to S phase. Therefore, the main difference between different viable attractors is the timing of the G1-S transition in comparison to other cell cycle processes such as mitosis, anaphase and cell division. This is also evident from Table 6, where the time to reach S phase varies significantly between many of the viable mutants. In fact, the majority of viable mutants affect the transition through S phase (as opposed to M phase), and so it appears that S phase pathways are more robustly designed with more alternative pathways. For example, one such alternative pathway is the Clb5 mediated degradation of CKI when Cln2 is not present in the cell.

Other unique dynamics are also captured by the results in Table 8. In particular, deletion of Yox1 / Yhp1 leads to early activation of the pathway involving Cln3. The model then predicts that this premature activation leads to the early degradation of CKI (and transition through S phase). For the Cdh1 mutant, the model undergoes cell division before Clb2 is fully degraded. Although the dynamics of Clb2 are not uniquely associated with this attractor (since it occurs in $P_A$), the effect does show up indirectly via Cdc20.



## 6 Discussion

In this paper, I have described a new Boolean network model of the *S. cerevisiae* cell cycle, which is consistent with a wide range of wild type and mutant phenotype data. The stable dynamics for the wild type and viable mutant models are remarkably robust, since (in each case) there is only one attractor for the dynamics to follow. The lack of alternative attractors demonstrates that the exact timing of events, and the order in which nodes update, does

not alter the fundamental behaviour of the system. i.e. cycling though the correct phases of the cell cycle in the correct order. Moreover, the stable dynamics are not affected by temporary perturbations to the states of any node. To see why this robustness is evident in this model, under suitable growth conditions, consider the roles of nodes S/MBF and Clb2. If Clb2 is inactive (as in G1 phase), then the only thing stopping S/MBF activation (via Cln3) is itself, by promoting Yox1 and Yhp1. Moreover, once S/MBF is active and has transcribed Cln2, Cln2 maintains S/MBF expression. This combination of negative and positive feedback is sufficient to initiate and maintain S/MBF (resp) and so trigger the inevitable chain of events that leads to DNA synthesis, Budding and Clb2 activation. The positive feedback loop involving Clb2 and SFF is then sufficient to trigger the following events (despite any variation in timings); inhibition of S/MBF, activation of Cdc20, FEAR, MEN, Cdc14 and Cdh1. Clb2 degradation and mitotic exit can then occur and return the cell to the normal G1 phase. The only things capable of breaking this inevitable cycle are the in built checkpoints. One thing to note here is that, even though S/MBF is self-activating in the model, this interaction is not necessary to observe this robustness and a model without this interaction still only has a single attractor (since the positive feedback loop between S/MBF and Cln2 is still functional). This observation of robustness in cell cycle regulation is one shared with previous studies (Li *et al* (2004); Braunewell & Bornholdt (2007)). In particular, Braunewell & Bornholdt (2007) showed that the existing Boolean model by Li *et al* (2004) maintained a suitable transition through the cell cycle despite stochastic fluctuations in process times.

This robustness in the synchronous deterministic model (in this paper) demonstrates that the synchronous updating scheme used is a suitable first approximation for this system. Moreover, the wild type and mutant attractors are all consistent with experimental data and provide a set of baseline results, to which more complicated updating schemes can be compared. Although not as precise as ODE models, the simple logical structure of this new model implies that it can be investigated in novel ways. For example, it is possible to use the wild type and checkpoint attractors to identify subsystems within the cell cycle, corresponding to different sub-networks with related dynamics. In this analysis, the full cell cycle could be partitioned into 7 distinguishable sub-networks (Fig.6A). Moreover, based on these sub-networks it is possible to produce a minimal 4-node model that underlies and drives the full cell cycle (Fig.6C,D and Table 7). It is interesting to note that this unbiased, automated method of identifying a core regulatory circuit, comes up with a similar network to that discussed / obtained independently by other authors. In particular, a manually described summary sub-network in Chen *et al* (2004) is based on 4 nodes, which match those found in this study.

Using new methods described in this paper, it was also possible to identify the main sub-dynamics that are conserved across the viable wild type and

mutant attractors. At the heart of these sub-dynamics are the genes / proteins involved in the transition into and out of mitosis, indicating that M phase is particularly tightly regulated. Conversely, S phase genes / proteins showed significantly more variability between viable mutants with the timing of Clb5 and CKI activation / deactivation particularly inconsistent. The fact that M phase might be more tightly regulated than S phase is backed up by the fact that more checkpoints are involved in regulating M phase events.

As mentioned earlier, mathematical models of the *S. cerevisiae* cell cycle have been produced, using both differential equations (Chen *et al* (2000, 2004); Queralt *et al* (2006); Barberis *et al* (2007); Tóth *et al* (2007)) and Boolean networks (Li *et al* (2004)). Many nodes and / or interactions in this model are similar to those in previous models, but there are also some significant differences. Firstly, genes and proteins that are part of the Yhp1 node (YHP1, YOX1, Yhp1, Yox1) were not included in any of the above mentioned models. This node provides added insight into the transition from M phase to G1 phase, in particular activation of the early G1 protein Cln3. In many of the previous models (Chen *et al* (2000, 2004); Li *et al* (2004); Barberis *et al* (2007)) activation of Cln3 is dependent on cell size. However, in Yox1$\triangle$ Yhp1$\triangle$ double mutants, the G1 to S transition begins when the cell is smaller (Pramila *et al* (2002)), indicating Cln3 becomes active when the cell is smaller. Cell size is obviously important for initiating the G1 to S phase transition, but these results predict that the timing of CLN3 transcription could also be a critical part of checkpoint regulating the G1 to S transition. This is consistent with studies indicating that other start checkpoint components regulate Whi5, which is downstream of Cln3 (Bernstein *et al* (2007)).

Another difference from other models, of the full cell cycle (Chen *et al* (2000, 2004); Li *et al* (2004)), is the activation of MEN and Cdc14 in M phase. In particular the involvement of FEAR components. In Chen *et al* (2004), activation of the MEN pathway (including Cdc15) is essentially independent of the FEAR pathway. However, experimental data suggests that the FEAR component Esp1 (separase) is essential for Tem1, Cdc15 and Cdc14 activation (Stegmeier *et al* (2002); D'Amours & Amon (2004); Queralt *et al* (2006) and so we have added this interaction accordingly. This is consistent with the approach taken with recent models of Mitotic exit (Queralt *et al* (2006); Tóth *et al* (2007)). In the existing Boolean model by Li *et al* (2004), no components of the MEN pathway are included.

Compared to the existing Boolean model (Li *et al* (2004)), the structure of the Boolean functions are quite different. Li *et al* (2004) used a general approach whereby a node $n_i$ only switches from 0 to 1 (at time $t$) if more in-neighbours (nodes with an edge going into $n_i$) activate than inhibit at time $t-1$. Similarly a node only switches from 1 to 0 if more in-neighbours inhibit than activate. However, this approach is inflexible and not suitable when the ef-

fect of one in-neighbour is dominant over another. In this new model, all the Boolean functions have been chosen to be consistent with the available data with some interactions being dominant over others. For example, Cdc14 is a single dominant activator of Cdh1 despite the fact that there are three inhibitor nodes (Cln2, Clb2 and Clb5). Additionally, activation and degradation delays have been incorporated into this new model but were not used in the existing Boolean model. These delays imply that the wild type and mutant attractors show greater resemblance to the biological system.

In the existing Boolean model (Li *et al* (2004)), nodes for ′Cell size′ and ′DNA replication′ are included but neither mitosis nor cell division are explicitly incorporated. Moreover, once the cell re-enters G1 phase, there is nothing (autonomous) in the model to trigger a new round of cell division, and consequently all the published attractors are fixed points. However, even when the model is adapted to resolve this issue and generate cyclic wild type behaviour, it is still inconsistent with a range of mutant phenotypes. In particular, inactivating Mcm1 / SFF in the Li *et al* (2004) model leads to a viable attractor (while the mutant is in reality inviable), whilst inactivating Cln2, Clb5, Swi5 and Sic1 leads to inviable attractors (while the mutants are in reality viable). My new model has incorporated mitosis and cell division into the model, as well as allowing Cln3 levels to rise autonomously to generate further rounds of cell division and generate cyclic attractors (i.e. the attractor covers a whole transition of the cell cycle). The new model is also consistent with the main mutant phenotypes associated with each node.

Although the model correctly captures the phenotypes of the wild type cell cycle and a number of key mutants, there is potential to improve the model by adding some extra nodes to capture extra important features. In this model, I have only included enough genes / proteins to represent the main features and phases of the cell cycle. However, extra genes and proteins involved in cell growth, budding, assembly of the mitotic spindle, chromosome alignment and sister chromatid separation could be included as more data become available. Moreover, in this model, single nodes often correspond to multiple genes and proteins, but the proteins within these groups have slightly distinct functions. The model may be improved by assigning the proteins to separate nodes, in order to capture these distinct functions. This approach may also allow the model to replicate further mutant phenotypes. Another way in which the model could better replicate wild type and mutant phenotypes, would be the inclusion of cell mass (as a discrete valued variable). This would allow the model to better represent the start and morphogenesis checkpoints, as well as mutant phenotypes that (a) alter cell size or (b) are dependant on the rate of cell growth (due to nutrients). A comprehensive description of mutant phenotypes can be found at http://mpf.biol.vt.edu/ (see also Chen *et al* (2004)).

As the cell grows, a bud forms from the side of the cell and eventually becomes

the daughter cell, after cell division occurs (the original cell being the mother cell). After the cell divides there are differences in gene expression in the two parts. In particular proteins Ace2 and Ash1 accumulate exclusively in the daughter cell but not in the original mother cell (Bähler (2005)). Taking into account such asymmetric behaviour can be another way of developing the model.

Finally, the model could be developed by assigning more accurate timings to specific interactions. In the model, the relative times taken to pass through each phase differ slightly from those in the real system. In particular, M phase takes longer than expected in the model, whilst S phase is shorter. This is due to the fact that there is a relatively large number of interactions in M phase (in this model), and since each of these must take at least one time step, the whole phase takes an artificially long time. Furthermore, general assumptions about transcription and degradation rates have been made but there is room to improve the model by fine tuning some of the times involved with particular interactions.



## Appendix

## A Incorporating time delays into Boolean functions

In this paper, I use a new technique that introduces 'dummy' nodes into a Boolean network model to represent time delays in certain interactions or 'signals'. Here, I describe how a model can be adapted to introduce *activation* and *degradation* delays to model (relatively) slow transcription and degradation. An accompanying example is given in Fig.1, Table 1 and Table 2.

Consider a node $n_b$ and the following interaction

- A set of neighbouring nodes $N_a = \{n_{a_1}, ..., n_{a_k}\}$ is involved in activating $n_b$ when they satisfy a logical condition $IN$

For example, in Fig.1C and Table 2, the logical condition used is $IN = (s_1 = 1$ OR $s_2 = 1)$.

Then, as previously mentioned, I want to model the following two types of delay

**A. Activation delay**

The set of nodes $N_a$ must satisfy $IN$ for $r_A$ continuous time steps (rather than the usual 1), in order for it to have an activating effect on $n_b$.

**B. Degradation delay**

If $n_b$ is already ON, then the activating effect due to $N_a$ remains until $IN$ is not satisfied for $r_D$ continuous time steps (rather than the usual 1).

In order to adapt the model to achieve this, I first add $r = \max\{r_A - 1, r_D - 1\}$ dummy nodes (with states $c_1$, ..., $c_r \in \{0, 1\}$) to the model with the following Boolean functions

**case** $i = 1$**:** $c_1 = 1$ IF $IN$ ($c_1 = 0$ otherwise)
**case** $i > 1$**:** $c_i = 1$ IF $c_{i-1} = 1$ ($c_i = 0$ otherwise)

Secondly, an additional response node $OUT$ (with state $c_{OUT}$) is added to the model with the Boolean function

$c_{OUT} = 1$ IF A OR B ($c_{OUT} = 0$ otherwise)

where

**A (Initial Activation) is**
$IN$ AND $c_1 = 1$ AND ... AND $c_{r_A-1} = 1$
**B (Maintenance) is**
$c_{OUT} = 1$ AND ($IN$ OR $c_1 = 1$ OR ... OR $c_{r_D-1} = 1$)

Finally the condition 'A OR B' replaces each occurrence of '$IN$' in the Boolean function $f_b$ of $n_b$.

An example incorporating such delays can be seen in Fig.1C and Table 2. The dynamics following the initiation and removal of this signal can be seen in Table 9.

Obviously, if there is no activation / degradation delay then $r_A$ / $r_D$ is equal to 1 and condition $A$ / $B$ is redundant (respectively). In the case, where there is no degradation delay, there is no need for the extra node $OUT$. Moreover, the extra $OUT$ node is not necessary if $IN$ is the only condition activating $n_b$. Instead, condition $B$ can be changed to

$s_b = 1$ AND ($IN$ OR $c_1 = 1$ OR ... OR $c_{r_D-1} = 1$)

This change can be applied to the above example, which leads to the following change in the Boolean function $f_4$ of $n_4$ (in Table 2).

- $s_4 = 1$ IF $s_3 = 0$ AND $IN$ AND $c_1 = 1$
- $s_4 = 1$ IF $s_3 = 0$ AND $s_4 = 1$ AND ($IN$ OR $c_1 = 1$ OR $c_2 = 1$)
  ($s_4 = 0$ otherwise)

Although, at first sight it seems an intensive way of introducing delays into the model, in reality many of the dummy nodes can be re-used in numerous

interactions. For example, if a transcription factor $X$ is involved in activating multiple genes / proteins, only one set of dummy nodes (and one OUT node) is required.

Obviously, the same techniques can be used to introduce other types of delay. For example, a straight activation delay could be achieved by allowing the condition $'c_{r_A-1} = 1'$ to replace each occurrence of $'IN'$ in the Boolean function $f_b$ (bypassing the $OUT$ node).

## B Dominant sub-dynamics

This section defines and describes how to identify *dominant sub-dynamics* from a Boolean network model. First, I give some preliminary definitions.

### *B.1 Partial state sequences*

For a subset of nodes $N \subseteq V$ consider the following definitions.

**Definition 1** *A* **partial state**, $\mathbf{x}^N \in \{0,1\}^{|N|}$ *is a set of Boolean states, one for each node* $n_i \in N \subseteq V$. *i.e.* $\mathbf{x}^N = \{s_i : n_i \in N\}$.

**Definition 2** *A* **partial state sequence**, $P = \{\mathbf{x}_0^N, \mathbf{x}_1^N, ..., \mathbf{x}_{q-1}^N\}$, *is an ordered set of partial states , for a node set* $N$ $(\subseteq V)$.

These *partial state sequences* can be used to represent sub-dynamics in Boolean network models and describe which attractors they occur in. For example, we can say that the partial state sequence $P_A$ in Fig.7 *conserved across* or *occurs in* in the wild type attractor (Fig.3A) since the partial states in $P_A$ cycle in the correct order within the wild type attractor. We note that the time taken to change from one partial state to the next is not considered since different processes can take different lengths of time under different conditions (compare $P_A$ in the WT and viable mutant attractors (Fig.4). More formally,

**Definition 3** *A partial state sequence* $P = \{\mathbf{x}_0^N, \mathbf{x}_1^N, ..., \mathbf{x}_{q-1}^N\}$ **conserved across** *or* **occurs in** *an attractor* $A = \{\mathbf{z}_0, ..., \mathbf{z}_{p-1}\}$ *if there exists integers* $b_0, ..., b_{p-1} \in \{0, ..., q-1\}$ *for which the following are true*

*(1)* *For* $k = 0, ..., p-1$, $\mathbf{x}_{b_k}^N = \{s_i \in \mathbf{z}_k : n_i \in N\}$.
*(2)* *For each* $k \in \{0, ..., p-1\}$ *and* $j = k-1 \pmod p$, *either*
***(a)*** $b_k = b_j$ *or* ***(b)*** $b_k = b_j + 1 \pmod q$
*(3)* *Properties 1 and 2 are not true for any smaller partial state sequence* $P' = \{\mathbf{y}_0^N, \mathbf{y}_1^N, ..., \mathbf{y}_{q'-1}^N\}$ *and integers* $c_0, ..., c_{p-1} \in \{0, ..., q'-1\}$ $(q' < q)$.

Returning to the previous example where $P_A$ occurs in the wild type attractor, the definition is satisfied by letting $p = 19$, $q = 6$ and choosing $b_k$s as follows

| $k$ | 0 | 1 | 2 | 3 | 4 | 5 | 6 | 7 | 8 | 9 | 10 | 11 | 12 | 13 | 14 | 15 | 16 | 17 | 18 |
|---|---|---|---|---|---|---|---|---|---|---|---|---|---|---|---|---|---|---|---|
| $b_k$ | 5 | 0 | 0 | 0 | 0 | 0 | 0 | 0 | 0 | 0 | 1 | 1 | 1 | 1 | 1 | 2 | 3 | 3 | 4 |

### *B.2 Dominant sub-dynamics*

In Irons & Monk (2007), *intersection sequences* were introduced to give an informative hierarchical breakdown of the global (stable) dynamics.

**Definition 4** *A partial state sequence $P$ for a node set $N$ is an* **intersection sequence***, if there exists a set of attractors $\mathbb{C}$ ($\subseteq \mathbb{A}$) for which the following hold*

*(1) $P$ occurs in every attractor $A \in \mathbb{C}$*
*(2) $P$ does not occur in any attractor $A \notin \mathbb{C}$*
*(3) Given a larger node set $M \supset N$, there is no partial state sequence $P'$ (for the node set $M$) that satisfies condition 1.*

*If the above properties hold, we say $P$* **intersects** *at $\mathbb{C}$.*

These sub-dynamics are useful for analysing the global dynamics since

(1) Each one is conserved across some set of attractors,
(2) Each one represents a breaking point in the stable dynamics. In particular, none can be enlarged with a node $n_i \notin N$ to produce a partial state sequence that still occurs in the same set of attractors.

These intersection sequences are used in Irons & Monk (2007) to break the attractors up in a hierarchical manner (*partition sequences*) and then identify *subsystems* that distinguish one level in the hierarchy from the next. However, as noted in Irons & Monk (2007), this method has one limitation in that it has difficulties with systems with lots of cyclic attractors, each one containing very similar (but not identical) sub-dynamics. For example, in the cell cycle model a significant number of different viable mutations lead to related (but not identical) cyclic sub-dynamics. Here,

(1) all of the attractors are cyclic,
(2) the primary differences between the attractors are the mutations,
(3) all of the attractors have very similar node sets responsible for the cyclic behaviour,
(4) all of the attractors correspond to the same function (transition through the cell cycle).

This leads to a situation where the main thing distinguishing the attractors are the mutations rather than the intersection sequences. Moreover, because of the similar dynamics in each attractor, lots of similar intersection sequences with overlapping nodes sets may occur in the same set of attractors. It is also debatable whether meaningful subsystems could be obtained from a set of mutant attractors because $n$ different systems are being considered for $n$ different mutants.

However, with the model described in this paper, it is still interesting to know what sub-dynamics are conserved across the viable attractors and which sub-dynamics distinguish the different viable mutant attractors. In order to do this we first filter out the less important informative intersection sequences. Firstly, since there may be multiple intersection sequences occurring in a particular set of attractors, we only keep those with the most nodes (*principle intersection sequence*). Secondly, we remove those that are just combinations of other principle intersection sequence to leave the *dominant sub-dynamics* used in this paper. More formally,

**Definition 5** *$P = \{\mathbf{x}_0^N, \mathbf{x}_1^N, ..., \mathbf{x}_{q-1}^N\}$ is a* **principle intersection sequence** *if there exists a set of attractors $\mathbb{C}$ ($\subseteq \mathbb{A}$) for which the following hold*

*(1) $P$ is an intersection sequence that intersects at $\mathbb{C}$.*
*(2) There is no intersection sequence $P'$ (for a node set $L$) for which*
  ***(a)*** *$\mid L \mid > \mid N \mid$*
  ***(b)*** *$P'$ occurs in every attractor $A \in \mathbb{C}$.*

**Definition 6** *$P = \{\mathbf{x}_0^N, \mathbf{x}_1^N, ..., \mathbf{x}_{q-1}^N\}$ is a* **dominant sub-dynamic** *if there exists a subset of attractors $\mathbb{C}$ ($\subseteq \mathbb{A}$) for which the following hold*

*(1) $P$ is a principle intersection sequence that intersects at $\mathbb{C}$.*
*(2) There is no set of principle intersection sequences $P'_1$, ..., $P'_k$ (involving node sets $M_1$, ..., $M_k$ resp) for which*
  ***(a)*** *$M_1 \cup ... \cup M_k \supseteq N$,*
  ***(b)*** *$P'_1$, ..., $P'_k$ all occur in every attractor $A \in \mathbb{C}$.*

### *B.3 Method for identifying dominant sub-dynamics*

All intersection sequences can be found using the method described in Irons & Monk (2007). Therefore, we just give the algorithm for finding all dominant sub-dynamics, given

**(a)** The complete set of attractors $\mathbb{A}$.
**(b)** The complete set of intersection sequences $P_1$, ...., $P_r$.

I assume each intersection sequence $P_i$ involves a node set $N_i$ and intersects at (occurs in) the set of attractors $\mathbb{C}_i$.

Stage 1 and 2 below will then find all *principle intersection sequence* and *dominant sub-dynamics* that satisfy Definitions 5 and 6 respectively.

### *B.3.1 Stage 1: Identifying all principle intersection sequences*

Initially, let the set $\mathbf{R} = \varnothing$ (empty set)

For every intersection sequence $P_i$ carry out the following steps.

**Step 1:** For each remaining intersection sequence $P_j \neq P_i$, check to see whether

**(a)** $\mid N_j \mid > \mid N_i \mid$
**(b)** $\mathbb{C}_j \supseteq \mathbb{C}_i$

If (a) and (b) are both satisfied, **break** and move on to the next intersection sequence $P_i$ (if there are any left).

**Step 2:** Add $P_i$ to the set $\mathbf{R}$

**end of procedure**

At the end of the procedure only those intersection sequences that satisfy property 2 of Definition 5 will ever reach step 2 and be added to the set $\mathbf{R}$. $\mathbf{R}$ will contain all principle intersection sequences at the end since, the procedure started with all intersection sequences and only intersection sequences can be principle intersection sequences (by property 1 of Definition 5).

### *B.3.2 Stage 2: Identifying all dominant sub-dynamics*

Initially, let the set $\mathbf{U} = \varnothing$ (empty set)

For every principle intersection sequence $P_i \in \mathbf{R}$ (from Stage 1), carry out the following steps.

**Step 1:** Let k = 0.

**Step 2:** For each remaining principle intersection sequence $P_j \neq P_i$ ($\in \mathbf{R}$), check to see whether $\mathbb{C}_j \supseteq \mathbb{C}_i$. If so,

- Increase k by 1
- Let $M_k = N_j$

**Step 3:** If k $> 0$ and $M_1 \cup ... \cup M_k \supseteq N_i$, **break** and move on to the next intersection sequence $P_i$ (if there are any left).

**Step 4:** Add $P_i$ to the set **U**

**end of procedure**

At the end of the procedure only those intersection sequences that satisfy property 2 of Definition 6 will ever reach step 4 and be added to the set **U** (all others are filtered out in steps 2 and 3). **U** will contain all dominant sub-dynamics at the end since, the procedure started with all principle intersection sequences and only intersection sequences can be dominant sub-dynamics (by property 1 of Definition 6).

## Role of the funding source

This work was supported by funding from BBSRC (grant ref: 02/B1/B/08370) and EPSRC (grant ref: EP/D003105/1).

## Acknowledgements

I would like to thank C. Cannings and N. Monk for critical reading of the manuscript and helpful comments.

## References

Albert, R., Othmer, H.G., 2003. The topology of the regulatory interactions predicts the expression pattern of the segment polarity genes in *Drosophila*. J. Theor. Biol. 223, 1–18.

Alexandru, G., Zachariae, W., Schleiffer, A., Nasmyth, K., 1999. Sister chromatid separation and chromosome re-duplication are regulated by different mechanisms in response to spindle damage. EMBO J. 18, 2707–2721.

Bähler, J., 2005. Cell-cycle control of gene expression in budding and fission yeast. Ann. Rev. Genet. 39, 69–94.

Barberis, M., Klipp, E., Vanoni, M., Alberghina, L., 2007. Cell size at S phase initiation: an emergent property of the $G_1$/S network. PLoS Comp. Biol. 3, e64.

Bernstein, K.A., Bleichert, F., Bean, J.M., Cross, F.R., Baserga, S.J., 2007. Ribosome biogenesis is sensed at the start cell cycle checkpoint. Mol. Biol. Cell. 18, 953–964.

Bloom, J., Cross, F.R., 2007. Multiple levels of cyclin specificity in cell-cycle control. Nat. Rev. Mol. Cell Biol. 8, 149–160.

Braunewell, S., Bornholdt, S., 2007. Superstability of the yeast cell-cycle dynamics: ensuring causality in the presence of biochemical stochasticity. J. Theor. Biol. 245, 638–643.

de Bruin, R.A.M., McDonald, W.H., Kalashnikova, T.I., Yates III, J., Wittenberg, C., 2004. Cln3 activates G1-specific transcription via phosphorylation of the SBF bound repressor Whi5. Cell. 117, 887–898.

Chaves, M., Albert, R., Sontag, E.D., 2005. Robustness and fragility of Boolean models for genetic regulatory networks. J. Theor. Biol. 235, 431–449.

Chaves, M., Sontag, E.D., Albert, R., 2006. Methods of robustness analysis for Boolean models of gene control networks. IEE Syst. Biol. 153, 154–167.

Chen, K.C., Csikasz-Nagy, A., Gyorffy, B., Val, J., Novak, B., Tyson, J.J., 2000. Kinetic analysis of a molecular model of the budding yeast cell cycle. Mol. Biol. Cell. 11, 369–391.

Chen, K.C., Calzone, L., Csikasz-Nagy, A., Cross, F.R., Novak, B., Tyson, J.J., 2004. Integrative analysis of cell cycle control in budding yeast. Mol. Biol. Cell. 15, 3841–3862.

Costanzo, M., Nishikawa, J.L., Tang, X., Millman, J.S., Schub, O., Breitkreuz, K., Dewar, D., Rupes I., Andrews, B., Tyers, M., 2004. CDK activity antagonizes Whi5, an inhibitor of G1/S transcription in yeast. Cell. 117, 899–913.

Cross, F.R., Archambault, V., Miller, M., Klovstad, M., 2002. Testing a mathematical model of the yeast cell cycle. Mol. Biol. Cell. 13, 52–70.

Csikász-Nagy, A., Battogtokh, D., Chen, K.C., Novák, B. Tyson, J.J., 2006. Analysis of a generic model of eukaryotic cell-cycle regulation. Biophys. J. 90, 4361-4379.

Cvrčková, F., Nasmyth, K., 1993. Yeast $G_1$ cyclins *CLN1* and *CLN2* and a GAP-like protein have a role in bud formation. EMBO J. 12, 5277-5286.

D'Amours, D., Amon, A., 2004. At the interface between signaling and execution of anaphase - Cdc14 and the FEAR network. Genes & Dev. 18, 2581–2595.

Epstein, C.B., Cross, F.R., 1992. CLB5: a novel B cyclin from budding yeast with a role in S phase. Genes & Dev. 6, 1695–1706.

Fauré, A., Naldi, A., Chaouiya, C., Thieffry, D., 2006. Dynamic analysis of a generic Boolean model for the control of the mammalian cell cycle. Bioinformatics. 22, 124–131.

Fraschini, R., Formenti, E., Lucchini, G., Piatti, S., 1999. Budding yeast Bub2 is localized at spindle pole bodies and activates the mitotic checkpoint via a different pathway from Mad2. J. Cell Biol. 145, 979–991.

Giaever, G., Chu, A.M., Ni, L., Connelly, C., Riles, L., Véronneau, S., Dow, S., Lucau-Danila, A., Anderson, K., André, B., Arkin, A.P., *et al*, 2002. Functional profiling of the *Saccharomyces cerevisiae* genome. Nature. 418, 387–391.

Henchoz, S., Chi, Y., Catarin, B., Herskowitz, I., Deshaies, R.J., Peter, M.

1997. Phosphorylation- and ubiquitin-dependent degradation of the cyclin-dependent kinase inhibitor Far1p in budding yeast. Genes & Dev. 11, 3046–3060.

Hood-DeGrenier, J.K., Boulton, C.N., Lyo, V., 2007. Cytoplasmic Clb2 is required for timely inactivation of the mitotic inhibitor Swe1 and normal bud morphogenesis in *Saccharomyces cerevisiae*. Curr. Genet. 51, 1–18.

Horak, C.E., Luscombe, N.M., Qian, J., Bertone, P., Piccirrillo, S., Gerstein, M., Snyder, M., 2002. Complex transcriptional circuitry at the G1/S transition in *Saccharomyces cerevisiae*. Genes & Dev. 16, 3017–3033.

Hu, F., Wang, Y., Liu, D., Li, Y., Qin, J., Elledge, S.J., 2001. Regulation of the Bub2/Bfa1 GAP complex by Cdc5 and cell cycle checkpoints. Cell. 107, 655-665.

Hu, F., Aparicio, O.M., 2005. Swe1 regulation and transcriptional control restrict the activity of mitotic cyclins toward replication proteins in *Saccharomyces cerevisiae*. PNAS. 102, 8910–8915.

Hwang, L.H., Lau, L.F., Smith, D.L., Mistrot, C.A., Hardwick, K.G., Hwang, E.S., Amon, A., Murray, A.W., 1998. Budding yeast Cdc20: a target of the spindle checkpoint. Science. 279, 1041–1044.

Irons, D.J., 2006. Improving the efficiency of attractor cycle identification in Boolean networks. Physica D. 217, 7–21.

Irons, D.J., Monk, N.A.M, 2007. Identifying dynamical modules from genetic regulatory systems: applications to the segment polarity network. BMC Bioinformatics 8:413.

Koch, C., Moll, T., Neuberg, M., Ahorn, H., Nasmyth, K., 1993. A role for the transcription factors Mbp1 and Swi4 in progression from G1 to S phase. Science. 261, 1551–1557.

Lee, K.S., Asano, S., Park, J-E., Sakchaisri, K., Erikson, R.L., 2005. Monitoring the cell cycle by multi-kinase-dependent regulation of Swe1/Wee1 in budding yeast. Cell Cycle. 4, 1346–1349.

Lew, D.J., 2003. The morphogenesis checkpoint: how yeast cells watch their figures. Curr. Opin. Cell Biol. 15, 648–653.

Li, X., Cai, M., 1999. Recovery of the yeast cell cycle from heat shock-induced $G_1$ arrest involves a positive regulation of $G_1$ cyclin expression by the S phase cyclin Clb5. J. Bio. Chem. 274, 24220–24231.

Li, F., Long, T., Ouyang, Q., Tang, C., 2004. The yeast cell-cycle is robustly designed. PNAS. 101, 4781–4786.

Li, S., Assmann, S.M., Albert, R., 2006. Predicting essential components of signal transduction networks: a dynamic model of guard cell abscisic acid signaling. PLoS Biol. 4, e312.

Liang F., Wang, Y., 2007. DNA damage checkpoints inhibit mitotic exit by two different mechanisms. Mol. Cell. Biol. 27, 5067–5078.

Lydall, D., Ammerer, G., Nasmyth, K., 1991. A new role for MCM1 in yeast: cell cycle regulation of SWI5 transcription. Genes & Dev. 5, 2405–2419.

Maher, M., Cong, F., Kindelberger, D., Nasmyth, K., Dalton, D., 1995. Cell cycle-regulated transcription of the *CLB2* gene is dependent on Mcm1 and

a ternary complex factor. Mol. Cell. Biol. 15, 3129–3137.

McKinney, J.D., Chang, F., Heintz, N., Cross, F.R., 1993. Negative regulation of FAR1 at the start of the yeast cell cycle. Genes & Dev. 7, 833–843.

Mendoza, L., Alvarez-Buylla, E.R., 1998. Dynamics of the genetic regulatory network for *Arabidopsis thaliana* flower morphogenesis. J. Theor. Biol. 193, 307–319.

Mortensen, E.M., Haas, W., Gygi, M., Gygi, S.P., Kellogg, D.R., 2005. Cdc28-dependent regulation of the Cdc5/Polo kinase. Curr. Biol. 15, 2033–2037.

Mura, I., Csikász-Nagy, A., 2008. Stochastic Petri Net extension of a yeast cell cycle model. J. Theor. Biol. 254, 850–860.

Musacchio, A., Salmon, D., 2007. The spindle-assembly checkpoint in space and time. Nat. Rev. Mol. Cell Biol. 8, 379–393.

Nash, P., Tang, X., Orlicky, S., Chen, Q., Gertler, F.B., Mendenhall, M.D., Sicheri, F., Pawson, T., Tyers. M., 2001. Multisite phosphorylation of a CDK inhibitor sets a threshold for the onset of DNA replication. Nature. 414, 514–521.

Nasmyth, K., Dirick, L., 1991. The role of SWI4 and SWI6 in the activity of G1 cyclins in yeast. Cell. 66, 995–1013.

Potapova, T.A., Daum, J.R., Pittman, D.B., Hudson, J.R., Jones, T.N., Satinova, D.L., Stukenberg, P.T, Gorbsky, G.J., 2006. The reversibility of mitotic exit in vertebrate cells. Nature. 440, 954–958.

Pramila, T., Miles, S., GuhaThakurta, D., Jemiolo, D., Breeden, L.L., 2002. Conserved homeodomain proteins interact with MADS box protein Mcm1 to restrict ECB-dependent transcription to the M/G1 phase of the cell cycle. Genes & Dev. 16, 3034–3045.

Pramila, T., Wu, W., Miles, S., Noble, W.S., Breeden, L.L., 2006. The Forkhead transcription factor Hcm1 regulates chromosome segregation genes and fills the S-phase gap in the transcriptional circuitry of the cell cycle. Genes & Dev. 20, 2266–2278.

Prinz, S., Hwang, E.S., Visintin, R., Amon, A., 1998. The regulation of Cdc20 proteolysis reveals a role for the APC components Cdc23 and Cdc27 during S phase and early mitosis. Curr. Biol. 8, 750–760.

Queralt, E., Lehane, C., Novak, B., Uhlmann, F., 2006. Downregulation of $PP2A^{Cdc55}$ phosphatase by separase initiates mitotic exit in budding yeast. Cell. 125, 719–732.

Richardson, H., Lew, D.J., Henze, M., Sugimoto, K., Reed, S.I., 1992. Cyclin-B homologs in *Saccharomyces cerevisiae* function in S phase and in G2. Genes & Dev. 6, 2021–2034.

Rudner, A.D., Murray, A.W., 2000. Phosphorylation by Cdc28 activates the Cdc20-dependent activity of the anaphase-promoting complex. J. Cell Biol. 149, 1377-1390.

Schwob, E., Nasmyth, K., 1993. CLB5 and CLB6, a new pair of B cyclins involved in DNA replication in *Saccharomyces cerevisiae*. Genes & Dev. 7, 1160–1175.

Schwob, E., Böhm, T., Mendenhall, M.D., Nasmyth, K., 1994. The B-type cy-

clin kinase inhibitor p40$^{SIC1}$ controls the G1 to S transition in *S. cerevisiae*. Cell. 79, 233-244.

Shirayama, M., Tóth, A., Gálová, M., Naysmyth, K., 1999. APC$^{Cdc20}$ promotes exit from mitosis by destroying the anaphase inhibitor Pds1 and cyclin Clb5. Nature. 402, 203–207.

Sidorova, J.M., Breeden, L.L., 1997. Rad53-dependent phosphorylation of Swi6 and down-regulation of CLN1 and CLN2 transcription occur in response to DNA damage in *Saccharomyces cerevisiae*. Genes & Dev. 11, 3032–3045.

Spellman, P.T., Sherlock, G., Zhang, M.Q., Iyer, V.R., Anders, K., Eisen, M.B., Brown, P.O., Botstein, D., Futcher, B., 1998. Comprehensive identification of cell cycle-regulated genes of the yeast *Saccharomyces cerevisiae* by microarray hybridization. Mol. Biol. Cell. 9, 3273–3297.

Stegmeier, F., Visintin, R., Amon, A., 2002. Separase, Polo kinase, the kinetochore protein Slk19, and Spo12 function in a network that controls Cdc14 localization during early anaphase. Cell. 108, 207–220.

Steuer, R. 2004. Effects of stochasticity in models of the cell cycle: from quantized cycle times to noise-induced oscillations. J. Theor. Biol. 228, 293–301.

Surana, U., Robitsch, H., Price, C., Schuster, T., Fitch, I., Futcher, A.B., Nasymth, K., 1991. The role of CDC28 and cyclins during mitosis in the budding yeast *S. cerevisiae*. Cell. 65, 145–161.

Tóth, A., Queralt, E., Uhlmann, F., Novák, B., 2007. Mitotic exit in two dimensions. J. Theor. Biol. 248, 560–573.

Tyers, M., Tokiwa, G., Nash, R., Futcher, B., 1992. The Cln3-Cdc28 kinase complex of *S. cerevisiae* is regulated by proteolysis and phosphorylation. EMBO J. 11, 1773–1784.

Verma, R., Feldman, R.M.R, Deshaies, R.J., 1997. SIC1 is ubiquitinated in vitro by a pathway that requires CDC4, CDC34 and cyclin/CDK activities. Mol. Biol. Cell. 8, 1427–1437.

Visintin, R., Craig, K., Hwang, E.S., Prinz, S., Tyers, M., Amon, A., 1998. The phosphatase Cdc14 triggers mitotic exit by reversal of Cdk-dependent phosphorylation. Mol. Cell. 2, 709–718.

Wäsch, R., Cross, F.R., 2002. APC-dependent proteolysis of the mitotic cyclin Clb2 is essential for mitotic exit. Nature. 418, 556–557.

Wijnen, H., Futcher, B., 1999. Genetic analysis of the shared role of CLN3 and BCK2 at the G1-S transition in *Saccharomyces cerevisiae*. Genetics. 153, 1131–1143.

Willems, A.R., Lanker, S., Patton, E.E., Craig, K.L., Nason, T.F., Mathias, N., Kobayashi, R., Wittenberg, C., Tyers, M., 1996. Cdc53 targets phosphorylated G1 cyclins for degradation by the ubiquitin proteolytic pathway. Cell. 86, 453–463.

Wittenberg, C., Reed, S.I., 2005. Cell cycle-dependent transcription in yeast: promoters, transcription factors, and transcriptomes. Oncogene. 24, 2746–2755.

Yeong, F.M., Lim, H.H., Padmashree, C.G., Surana, U., 2000. Exit from mito-

sis in budding yeast: biphasic inactivation of the Cdc28-Clb2 mitotic kinase and the role of Cdc20. Mol. Cell. 5, 501-511.

Zachariae, W., Schwab, M., Nasmyth, K., Seufert, W. 1998. Control of cyclin ubiquitination by CDK-regulated binding of Hct1 to the Anaphase Promoting Complex. Science. 282, 1721–1724.

Zhang, Y., Qian, M., Ouyang. Q., Deng, M., Li, F., Tang, C. 2006. Stochastic model of yeast cell-cycle network. Physica D. 219, 35–39.

Table 1
Example Boolean function for the network in Fig.1B

| Node | Conditions that ensure node takes state 1 |
|---|---|
| $n_4$ | $s_3 = 0$ AND ($s_1 = 1$ OR $s_2 = 1$) |

Condition (at time $t-1$) that leads to that node taking state 1 a time $t$. If the condition is not met then it takes state 0 at time $t$.



Table 2
Boolean functions associated with the adapted network in Fig.1C.

| Node | Conditions that ensure node takes state 1 |
|---|---|
| $d_1$ | $IN$ |
| $d_2$ | $c_1 = 1$ |
| $OUT$ | $IN$ AND $c_1 = 1$ |
| | $c_{OUT} = 1$ AND ($IN$ OR $c_1 = 1$ OR $c_2 = 1$) |
| $n_4$ | $s_3 = 0$ AND $IN$ AND $c_1 = 1$ |
| | $s_3 = 0$ AND $c_{OUT} = 1$ AND ($IN$ OR $c_1 = 1$ OR $c_2 = 1$) |

Boolean functions after time delays have been added (to the Boolean function in Table 1). Here, the logical condition $IN = (s_1 = 1$ OR $s_2 = 1)$, is subject to activation and degradation delays ($r_A = 2$ and $r_D = 3$). Each row represents a condition (at time $t-1$) that can lead to that node taking state 1 a time $t$. If no such condition is met for a particular node then it takes state 0 at time $t$. $c_1$, $c_2$ and $c_{OUT}$ correspond to the states of the new nodes $d_1$, $d_2$ and $OUT$ (resp).

Table 3
Boolean functions for the 18 nodes in the new cell cycle model

| **Node** | **Conditions that ensure node takes state 1** | **Interactions** |
|---|---|---|
| Cln3 | [Yhp1 = 0]{2:1} | $\bar{H}$ |
| S/MBF | Clb2 = 0 AND (Cln3 = 1 OR Cln2 = 1 OR S/MBF = 1) | $\bar{M} \wedge (A \vee Y)$ |
| Cln2 | [S/MBF = 1]{2:1} | $B$ |
| Clb5 | Cdc20 = 0 AND [S/MBF = 1]{4:1} | $\bar{O} \wedge B \quad (slow)$ |
| | Cdc20 = 0 AND CKI = 0 AND [S/MBF = 1]{2:3} | $\bar{O} \wedge \bar{V} \wedge B \quad (fast)$ |
| Yhp1 | [S/MBF = 1]{2:6} | $G$ |
| Clb2 | CKI = 0 AND Cdh1 = 0 AND B = 1 | $\bar{U} \wedge \bar{V} \wedge (I \vee J)$ |
| | CKI = 0 AND Cdc20 = 0 AND B = 1 | |
| | CKI = 0 AND Cdh1 = 0 AND Clb2 = 1 AND SFF = 1 | |
| | CKI = 0 AND Cdc20 = 0 AND Clb2 = 1 AND SFF = 1 | |
| SFF | CKI = 0 AND Cdh1 = 0 AND B = 1 | $(\bar{U} \wedge \bar{V} \wedge J) \vee I$ |
| | CKI = 0 AND Cdc20 = 0 AND B = 1 | |
| | Clb2 = 1 AND SFF = 1 | |
| Cdc20 | M = 1 AND Clb2 = 1 AND [SFF = 1]{2:1} | $L \wedge N$ |
| FEAR | Cdc20 = 1 | $P$ |
| MEN | FEAR = 1 AND Clb2 = 1 | $Q$ |
| Cdc14 | FEAR = 1 AND MEN = 1 | $R$ |
| Swi5 | Clb2 = 0 AND [SFF = 1]{2:3} | $L \wedge (\bar{M} \vee S)$ |
| | Cdc14 = 1 AND [SFF = 1]{2:3} | |
| CKI | [Cdc14 = 1 AND Swi5 = 1]{2:1} | $(S \wedge T) \vee (\bar{C} \wedge (T \vee Y))$ |
| | Cln2 = 0 AND Clb5 = 0 AND Clb2 = 0 AND [Swi5 = 1]{2:1} | |
| | Cln2 = 0 AND Clb5 = 0 AND Clb2 = 0 AND CKI = 1 | |
| Cdh1 | Cdc14 = 1 | $\bar{D} \vee S$ |
| | Cln2 = 0 AND Clb5 = 0 AND Clb2 = 0 | |
| S | CD = 0 AND S = 1 | $\bar{X} \wedge (E \vee Y)$ |
| | CD = 0 AND [(Clb5 = 1 OR Clb2 = 1)]{2:1} | |
| B | CD = 0 AND B = 1 | $\bar{X} \wedge (F \vee Y)$ |
| | CD = 0 AND [(Cln2 = 1 OR Clb5 = 1)]{6:1} | |
| M | CD = 0 AND M = 1 | |
| | CD = 0 AND [S = 1 AND Clb2 = 1]{2:1} | $\bar{X} \wedge (K \vee Y)$ |
| CD | CD = 0 AND [M = 1 AND FEAR = 1 AND Cdc14 = 1]{2:1} | $\bar{X} \wedge W$ |

Column 2: Each row represents a condition (at time $t-1$) that can lead to that node taking state 1 a time $t$. If no such condition is met for a particular node then it takes state 0 at time $t$. $'[Condition]\{r_A : d_A\}'$ implies that the interaction is subject to activation and degradation times of $r_A$ and $d_A$ respectively instead of the usual 1 (discussed in text). Activation and degradation times are 1 unless otherwise specified. Column 3: How interactions (**A** - **Y** from text) combine to give Boolean functions. Logical operations are AND ($\wedge$), OR ($\vee$) and NOT (e.g. $\bar{H}$ implies NOT $H$).

Table 4
Genes, proteins and events associated with each node in the model

| **Node** | **Associated genes, proteins and events** |
|---|---|
| Cln3 | CLN3, Cln3-Cdc28, Bck2 |
| S/MBF | SBF (Swi6-Swi4), MBF (Swi6-Mbp1) |
| Cln2 | CLN1, CLN2, Clb1-Cdc28, Clb2-Cdc28 |
| Clb5 | CLB5, CLB6, Clb5-Cdc28, Clb6-Cdc28 |
| Yhp1 | YHP1, YOX1, Yhp1, Yox1 |
| Clb2 | CLB1, CLB2, Clb1-Cdc28, Clb2-Cdc28 |
| SFF | Fkh2, Mcm1, Ndd1 |
| Cdc20 | CDC20, Cdc20, APC |
| FEAR | Pds1 (securin), Esp1 (Separase), Fob1, Slk19, Spo12 |
| MEN | Tem1, Cdc15, Cdc5, Bub2, Bfa1, Lte1, Dbf1, Mob1 |
| Cdc14 | Cdc14, Net1 |
| Swi5 | SWI5, Swi5 |
| CKI | SIC1, Sic1, Cdc6 |
| Cdh1 | Cdh1, APC |
| S | DNA synthesis |
| B | Bud formation, Swe1 degradation |
| M | Entry to Mitosis |
| CD | Cell Division |

Table 5
Experimental data corresponding to the *S. cerevisiae* mutants associated with each node.

| Node | Mutant | Phenotype | Reference |
|---|---|---|---|
| Cln3 | Cln3△, Bck2△ | Inviable, G1 arrest | Chen *et al* (2004) † |
| S/MBF | Swi4△, Swi6△ | Inviable, G1 arrest | Nasmyth & Dirick (1991); Koch *et al* (1993) |
| | Swi4△, Mbp1△ | Inviable, G1 arrest | Koch *et al* (1993); Wijnen & Futcher (1999) |
| Cln2 | Cln1△, Cln2△ | Viable, large cell size | Chen *et al* (2004) † |
| Clb5 | Clb5△, Clb6△ | Viable, long G1 phase | Chen *et al* (2004) † |
| Yox1 | Yox1△, Yhp1△ | Viable, short G1 phase | Pramila *et al* (2002) |
| Clb2 and SFF | Clb1△, Clb2△ | Inviable, G2 arrest | Chen *et al* (2004) † |
| Cdc20 | Cdc20△ | Inviable, M arrest | Chen *et al* (2004) † |
| FEAR | Esp1△ | Inviable, M arrest | Chen *et al* (2004) † |
| MEN | Tem1△ | Inviable, M arrest | Chen *et al* (2004) † |
| | Cdc15△ | Inviable, M arrest | Chen *et al* (2004) † |
| Cdc14 | Cdc14△ | Inviable, M arrest | Chen *et al* (2004) † |
| Swi5 | Swi5△ | Viable, short G1 phase | Chen *et al* (2004) † |
| CKI | Sic1△ , Cdc6△ | Viable, short G1 phase | Chen *et al* (2004) † |
| Cdh1 | Cdh1△ | Viable | Giaever *et al* (2002) ⋆ |

† : Chen *et al* (2004) considered the viability of numerous mutations, the data for which is stored at http://mpf.biol.vt.edu/research
⋆ : data stored in database at http://db.yeastgenome.org/ from genome wide study by Giaever *et al* (2002).

Table 6
Table showing the effect of permanently fixing node states to 0, in the Boolean network model described in Table 3.

| Node(s) | Viability of main attractor | Size of main attractor | Time to reach S |
|---|---|---|---|
| WT | Viable | 19 | 8 |
| Cln3 | Inviable, G1 arrest | 1 | n/a |
| S/MBF | Inviable, G1 arrest | 1 | n/a |
| Cln2 | Viable | 21 | 8 |
| Clb5 | Viable | 20 | 12 |
| Yhp1 | Viable | 18 | 7 |
| Clb2 and SFF | Inviable, G2 arrest | 1 | n/a |
| Cdc20 | Inviable, M arrest | 1 | n/a |
| FEAR | Inviable, M arrest | 1 | n/a |
| MEN | Inviable, M arrest | 1 | n/a |
| Cdc14 | Inviable, M arrest | 1 | n/a |
| Swi5 | Viable | 19 | 6 |
| CKI | Viable | 19 | 6 |
| Cdh1 | Viable | 20 | 9 |

For each mutant model, the viability and size of the main attractor is given. For viable attractor cycles, the length of G1 and S phase is also given, which is the number of time steps between activation of CD (Cell division) and S (DNA synthesis). Wild type data (no fixed states) is given for comparison purposes. All mutant attractors are shown in Fig.4.

Table 7
Boolean functions for the 4 nodes in the reduced model in Fig.6C.

| **Node** | **Conditions that ensure node takes state 1** |
|---|---|
| S/MBF | Clb2 = 0 |
| Clb2 | Cdc20 = 0 AND CKI = 0 |
| Cdc20 | Clb2 = 1 |
| CKI | Cdc20 = 1 |
| | SBF = 0 AND Clb2 = 0 AND CKI = 1 |

Each row represents a condition (at time $t-1$) that can lead to that node taking state 1 at time $t$. If no such condition is met for a particular node then it takes state 0 at time $t$.

Table 8
Table showing the nodes whose dynamics are uniquely associated with each viable attractor.

| **Model** | **Attractor specific dynamics** |
|---|---|
| Wild Type | Clb5, Swi5, CKI |
| Cln2 mutant | Cln2, Clb5, Swi5, CKI |
| Clb5 mutant | Clb5, Yhp1, CKI, S |
| Yhp1 mutant | Cln3, Clb5, Yhp1, CKI, S |
| Swi5 and CKI mutants $\star$ | Clb5, Swi5, CKI |
| Cdh1 mutant | Clb5, Cdc20, CKI, Cdh1 |

$\star$: Swi5 mutation inactivates CKI. The dynamics of Clb5 are equivalent in both Swi5 and CKI mutants

Table 9
Dynamics associated with the example model in Fig.1C and Table 2, following initiation and removal of a signal from $n_1$.

| | $\mathbf{n_1}$ | $\mathbf{n_2}$ | $\mathbf{n_3}$ | $\mathbf{d_1}$ | $\mathbf{d_2}$ | **OUT** | $\mathbf{n_4}$ |
|---|---|---|---|---|---|---|---|
| | 0 | 0 | 0 | 0 | 0 | 0 | 0 |
| $\mathbf{n_1}\uparrow$ | 1 | 0 | 0 | 0 | 0 | 0 | 0 |
| | 1 | 0 | 0 | 1 | 0 | 0 | 0 |
| | 1 | 0 | 0 | 1 | 1 | 1 | 1 |
| | ... | ... | ... | ... | ... | ... | ... |
| | 1 | 0 | 0 | 1 | 1 | 1 | 1 |
| $\mathbf{n_1}\downarrow$ | 0 | 0 | 0 | 1 | 1 | 1 | 1 |
| | 0 | 0 | 0 | 0 | 1 | 1 | 1 |
| | 0 | 0 | 0 | 0 | 0 | 1 | 1 |
| | 0 | 0 | 0 | 0 | 0 | 0 | 0 |
| | ... | ... | ... | ... | ... | ... | ... |

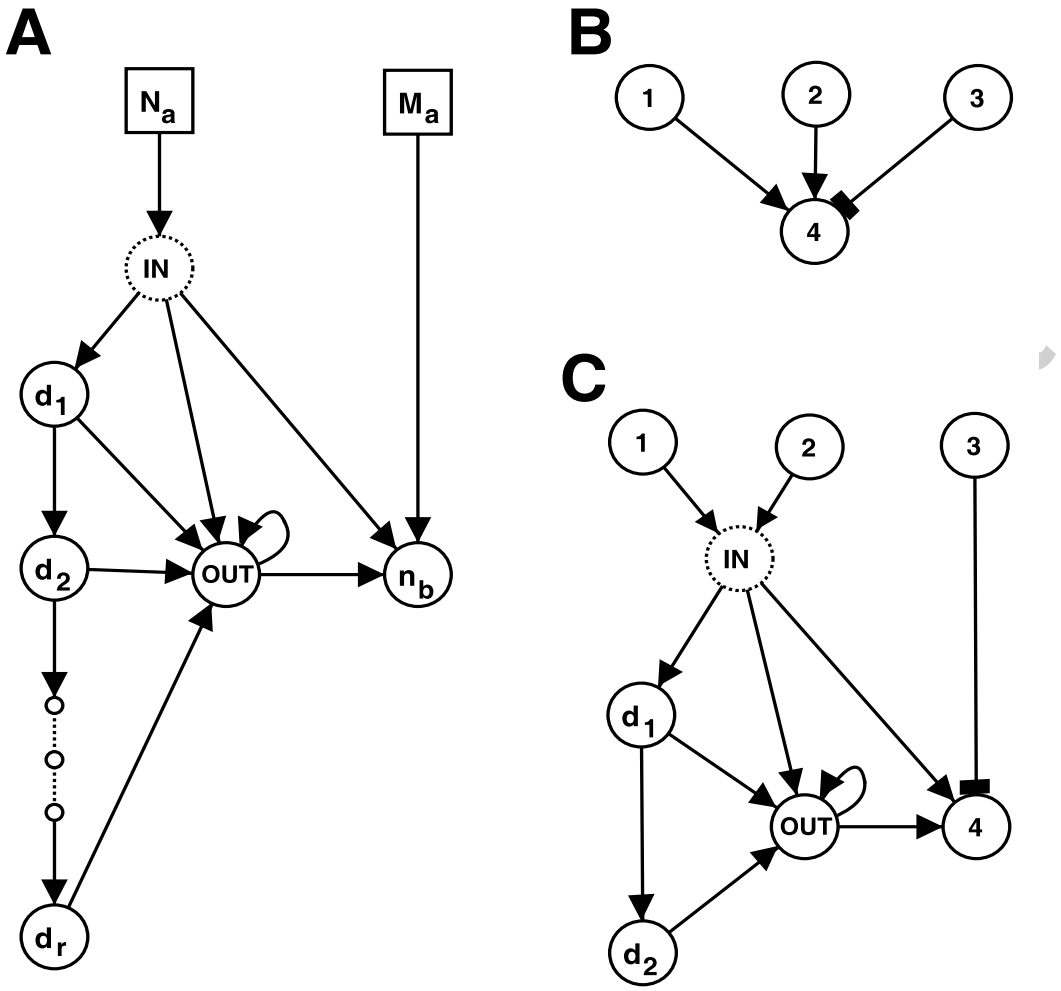


Fig. 1. Example demonstrating the network modifications when a time delay is added to a Boolean network model. (A) The general case where an interaction between nodes $N_a = \{n_{a_1}, ..., n_{a_k}\}$ and $n_b$ is delayed by $r$ time steps. $M_a$ is any set of nodes that are involved in other (non delayed) interactions. $d_1$, ..., $d_r$, $OUT$ are extra nodes added to the model (with Boolean functions described in Appendix A). $IN$ corresponds to the signal from / state of $N_a$ and is NOT an extra node. (B,C) Example where the signal from $N_a = \{1,2\}$ to $n_b = \{4\}$, represented by a logical condition $IN = (s_1 = 1 \text{ OR } s_2 = 1)$, is subject to activation and degradation delays (accompanying Boolean functions are given in Table 2). Activation and degradation of this signal takes 2 and 3 time steps (resp).

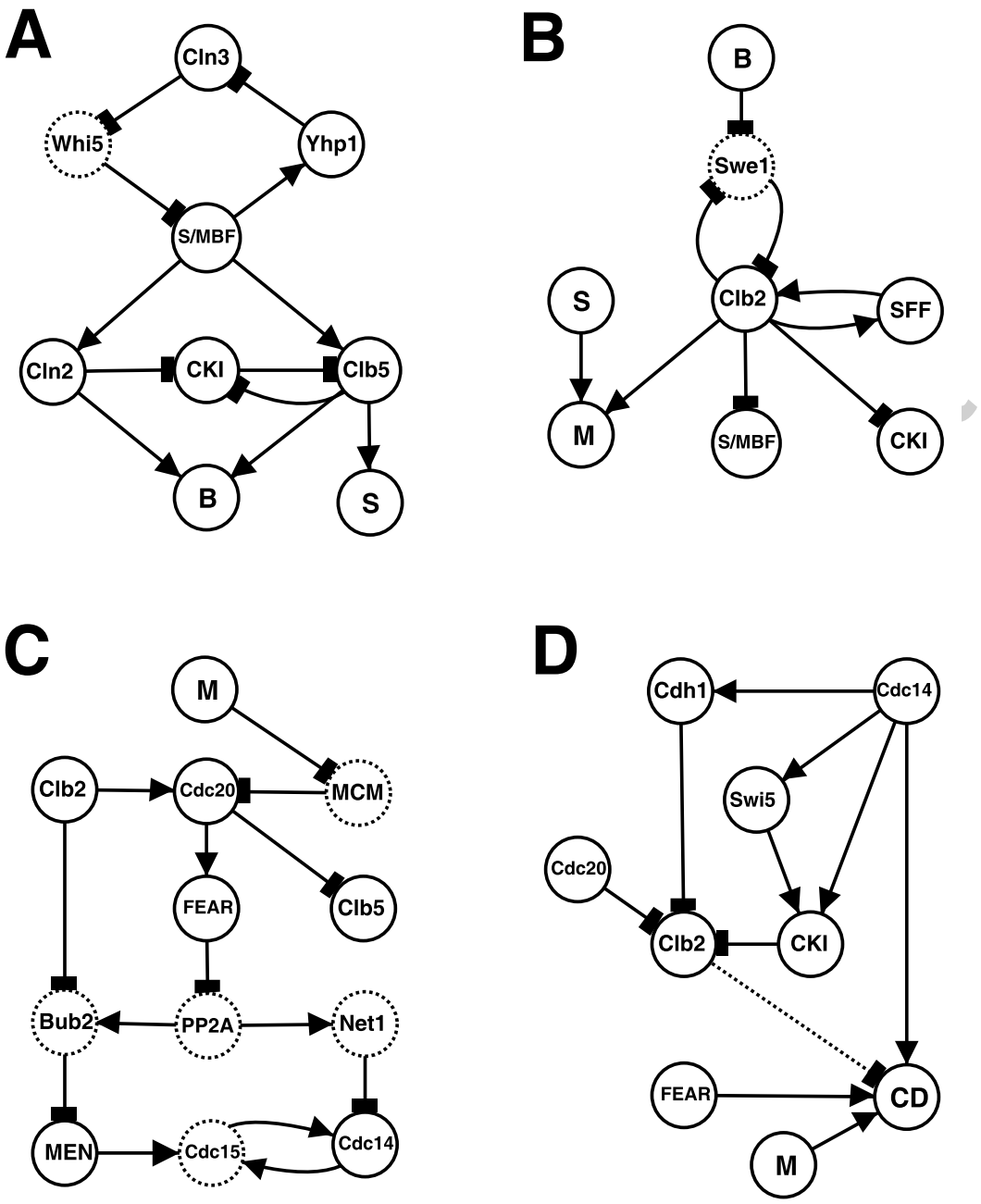


Fig. 2. Main interactions involved in different phases of the cell cycle. (A) Transition from G1 to S phase. (B) Entry into Mitosis. (C) Transition through M phase and execution of Anaphase. (D) Exit from Mitosis. Boolean functions for the main nodes (solid outline) are described in Table 3, whilst a summary of the main interactions is given in the text. Dashed nodes and lines correspond to genes / proteins or interactions that are not explicitly included in the model, but incorporated within the Boolean functions of neighbouring nodes.

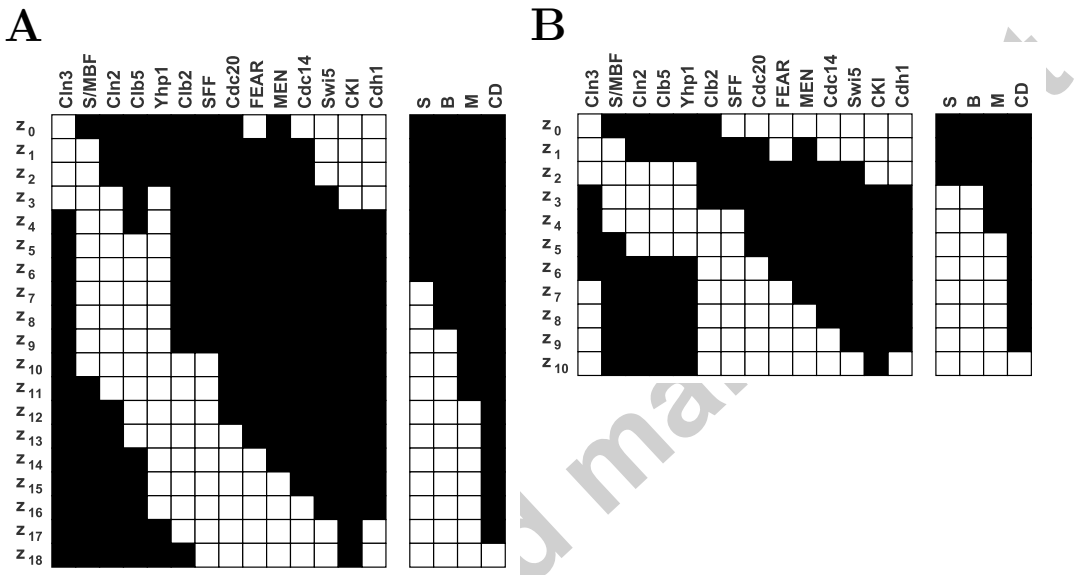


Fig. 3. Attractors associated with the Boolean network model described in Table 3 . Each column corresponds to a node in the model, whilst each row corresponds to an attractor state. White / Black corresponds to the node having state 1 / 0. The model runs through the attractor states in a cyclic fashion over time. (A) Wild Type attractor. (B) Wild type attractor for an equivalent model without additional time delays. To do this, the *slow* function for Clb5 was chosen over the *fast* one, so that S/MBF can activates Clb5 in the presence of CKI.

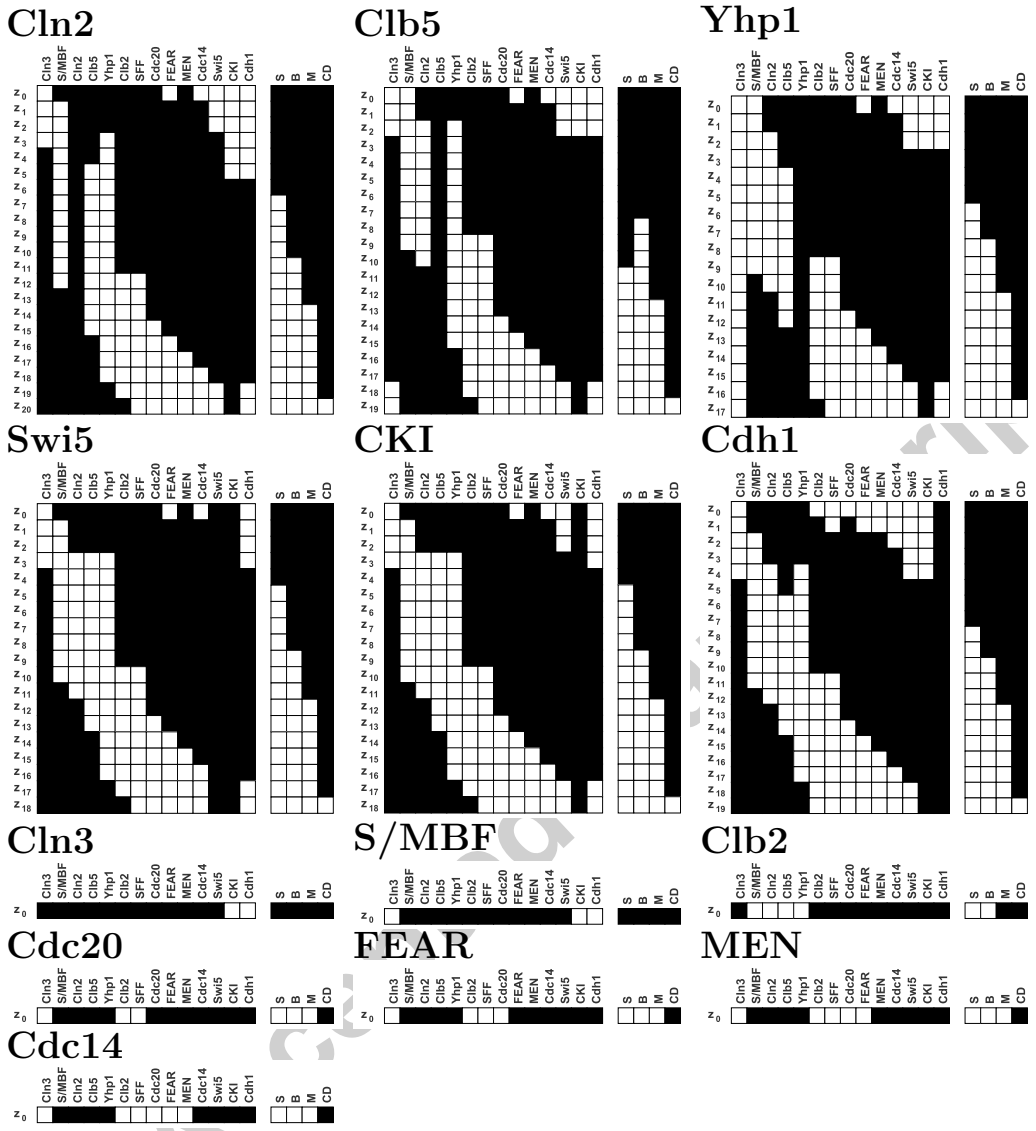


Fig. 4. Main attractors for each mutant phenotype. Each column corresponds to a node in the model, whilst each row corresponds to an attractor state. White / Black corresponds to the node having state 1 / 0. For cyclic attractors, the model runs through the attractor states in a cyclic fashion over time. For each mutant model, the following % of initial conditions converge to this main attractor (based on a sample of 1,000,000 initial states). Cln2: 100%. Clb5: 100%. Yhp1: 100%. Swi5: 100%. CKI: 100%. Cdh1: 100%. Cln3: 83.4%. S/MBF: 62.4%. Clb2: 86.4%. Cdc20: 88.7%. FEAR: 89.4%. MEN: 89.3%. Cdc14: 89.1%.

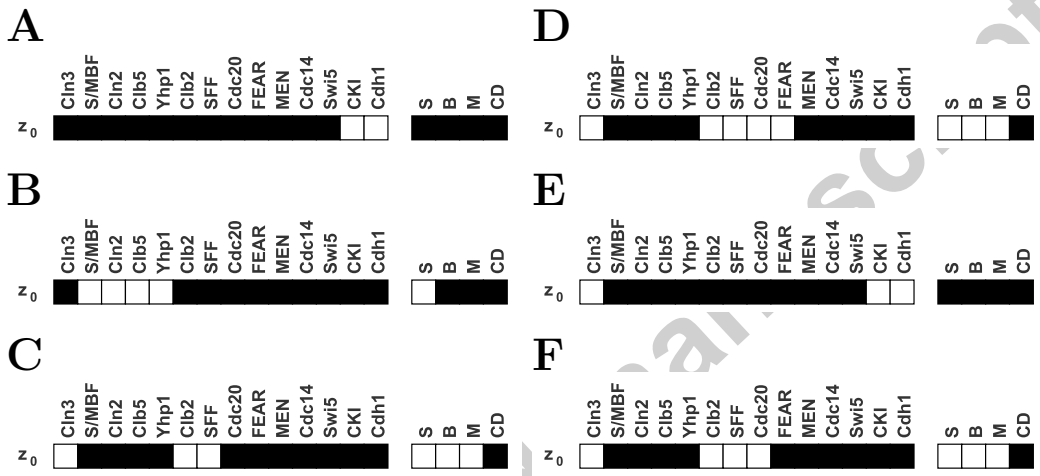


Fig. 5. Attractors associated with checkpoint activation, for the Boolean network described in Table 3 (discussed in text). Each column corresponds to a node in the model, whilst each row corresponds to an attractor state. White / Black corresponds to the node having state 1 / 0. (A) Attractor for response to the start checkpoint. (B) Attractor for response to the morphogenesis checkpoint. (C,D) Attractor for response to two different spindle assembly checkpoints. (E,F) Attractor for the response to two different DNA damage checkpoints.

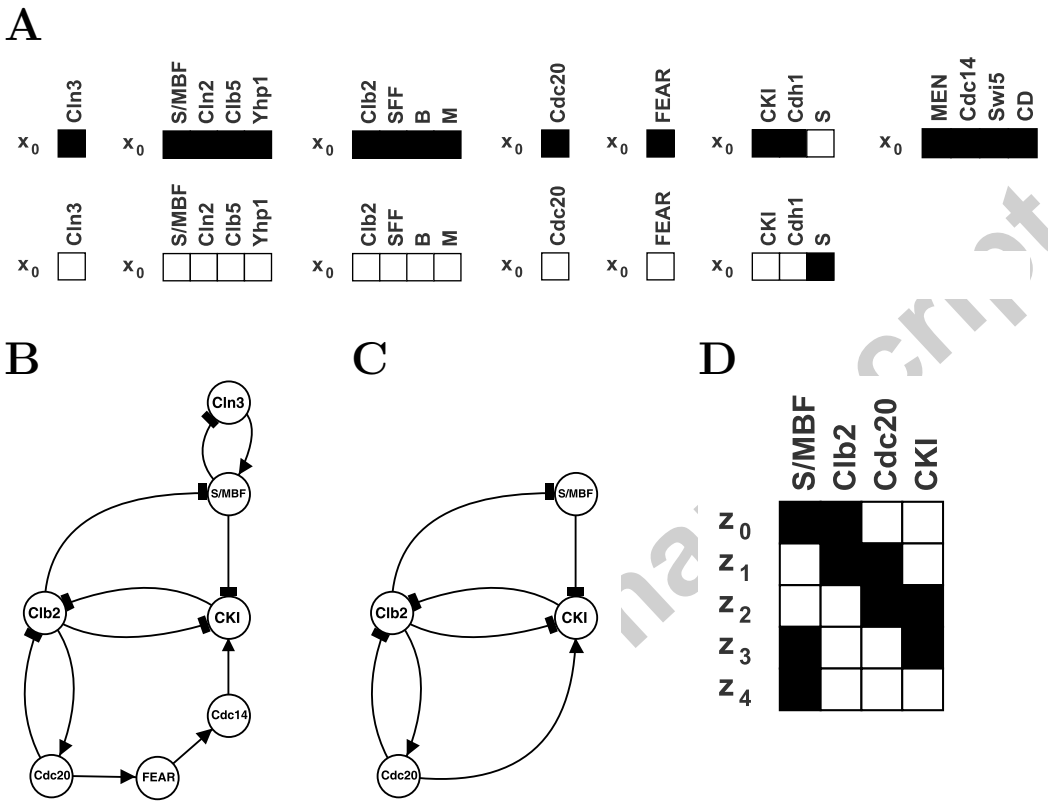


Fig. 6. Model reduction from the original Boolean model (A) Subsystems identified from the wild type model (checkpoint attractors). These subsystems partition the system into 7 subnetworks. (B,C) Reduced models based on the sub-networks from A, where one gene / protein is manually chosen to represent each of the sub-networks. The main features of the reduced model in B can be captured by the core network in C. (D) Attractor for the model in C, with Boolean functions in Table 7. In A and D, each column corresponds to a node in the model, whilst each row corresponds to a state. White / Black corresponds to the node having state 1 / 0. In D, the model runs through the attractor states in a cyclic fashion over time.

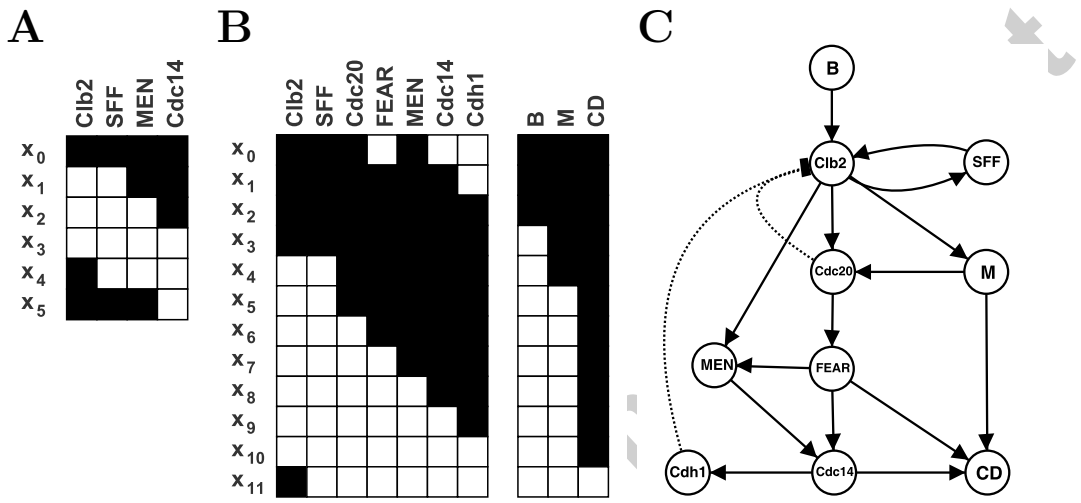


Fig. 7. Sub-dynamics conserved across multiple wild type and mutant viable attractors. (A,B) Each column corresponds to a node in the model, whilst each row corresponds to a state for the nodes. White / Black corresponds to the node having state 1 / 0. (A) Sub-dynamic conserved across all 7 viable attractors. (B) Sub–dynamic conserved across 6 of 7 viable attractors (all except Cdh1$\triangle$). (C) Main interactions involved in the sub-dynamic in B. Positive interactions activating the cascade are shown in bold, whilst the main inhibitory interactions between nodes are dashed.